Dalton Transactions

RSC Publishing

PAPER

View Article Online
View Journal | View Issue

Cite this: *Dalton Trans.*, 2013, **42**, 6495

Heterolytic activation of dihydrogen by platinum and palladium complexes†‡

Karina Q. Almeida Leñero,[a,e] Yannick Guari,[b,f] Paul C. J. Kamer,*[a,c] Piet W. N. M. van Leeuwen,*[a,g] Bruno Donnadieu,[b] Sylviane Sabo-Etienne,[b] Bruno Chaudret,[b] Martin Lutz[d] and Anthony L. Spek[d]

Wide bite angle diphosphine ligands were used to prepare [(diphosphine)M(2-(diphenylphosphino)-pyridine)]$^{2+}$ complexes (M = Pd, Pt). Except for the ligand with the largest bite angle, 2-(diphenylphosphino)pyridine coordinates in a bidentate mode leading to bis-chelate complexes. In the case of Xantphos (9,9-dimethyl-4,5-bis(diphenylphosphino)-xanthene, β_n = 111°) two types of complexes are formed, in which 2-(diphenylphosphino)pyridine coordinates in a mono- or bidentate fashion, respectively. The crystal structures of three of the Pt complexes were determined. The X-ray crystal structure of [(Xantphos)-Pt(2-(diphenylphosphino)pyridine)]$^{2+}$ shows that Xantphos coordinates in a tridentate P,O,P fashion. Under dihydrogen pressure, the pyridyl moiety in the platinum complexes can de-coordinate to provide a vacant coordination site at the metal center. Furthermore it can act as an internal base to assist the heterolytic cleavage of dihydrogen. The reaction yields a platinum hydride with a protonated pyridine moiety in close proximity to one another. The structure as well as the reactivity of the complexes towards dihydrogen is governed by the steric requirements of the diphosphines. The crystal structure of [(dppf)-PtH(2-(diphenylphosphino)pyridinium)](OTf)$_2$ has been determined. Palladium complexes containing DPEphos or Xantphos decompose under dihydrogen pressure. In the case of dppf slow heterolytic splitting of dihydrogen occurs to form the hydride complex [(dppf)PdH(2-(diphenylphosphino)pyridinium)]-(OTf)$_2$ which contains a protonated 2-(diphenylphosphino)pyridine ligand. In solution, this compound slowly undergoes P–C bond cleavage of the 2-(diphenylphosphino)pyridine ligand to form [(dppf)Pd-(PHPh$_2$)(η^1-C$_5$H$_4$NH)](OTf)$_2$. When the 6-methyl-2-pyridyldiphenylphosphine ligand is used, the reaction of the palladium complex with dihydrogen is very fast and the hydride complex immediately rearranges to the diphenylphosphino compound resulting from P–C bond cleavage.

Received 9th October 2012,
Accepted 7th January 2013

DOI: 10.1039/c3dt32395a

www.rsc.org/dalton

Introduction

The activation of HX molecules (X = H, SiR$_3$) by transition metal complexes is a key step in the mechanism of many catalytic reactions.[1–3] It can either occur *via* oxidative addition involving a sigma-complex or not, for example in catalytic hydrogenation, hydroformylation or hydrosilylation, or *via* heterolytic cleavage as in processes such as hydrogen metabolism,[4–6] nitrogen fixation[7] or D$_2$/H$^+$ exchange (Fig. 1).[8–10]

The heterolytic activation of HX is usually achieved using metal centers in medium or high oxidation states and requires the assistance of a Brønsted base. Some ligands act as intramolecular bases to assist the splitting of H$_2$, which has been reported for complexes containing sulfides,[11] thiolates,[8a,12] amines,[13] or nitrosyl groups.[14] During the cleavage of the HX bond the main interaction involved is σ donation from HX to an empty d orbital of the metal. Another important interaction that sometimes occurs prior to the H–X bond splitting is a proton–hydride interaction, or dihydrogen bonding.[15–18] The

[a]*Van't Hoff Institute for Molecular Sciences, Universiteit van Amsterdam, Nieuwe Achtergracht 166, 1018 WV Amsterdam, The Netherlands. E-mail: pcjk@st-andrews.ac.uk, PvanLeeuwen@iciq.es*
[b]*CNRS, LCC (Laboratoire de Chimie de Coordination), 205 route de Narbonne, BP 44099, F-31077 Toulouse Cedex 4, France*
[c]*EaStCHEM, Department of Chemistry, St. Andrews University, St. Andrews, Scotland, UK*
[d]*Bijvoet Center for Biomolecular Research, Crystal and Structural Chemistry, Utrecht Univerity, Padualaan 8, 3584 CH Utrecht, The Netherlands*
[e]*Shell Technology Centre Thornton, P.O. Box 1, Chester CH1 3SH, UK*
[f]*Université Montpellier II, Place Eugène Bataillon, 34095 Montpellier, France*
[g]*Institute of Chemical Research of Catalunia (ICIQ), Av. Piasos Catalans 16, 43007 Tarragona, Spain*

†Dedicated to Professor David Cole-Hamilton, a great scientist and even greater friend.

‡Electronic supplementary information (ESI) available: Dihydrogen bonding and hydrogenation studies, CIF files giving crystal data for **Pt1b**, **Pt1c**, ***trans*1d** and **Pt2a-Me**. CCDC 904331, 904332, 904333, 904334. For ESI and crystallographic data in CIF or other electronic format see DOI: 10.1039/c3dt32395a

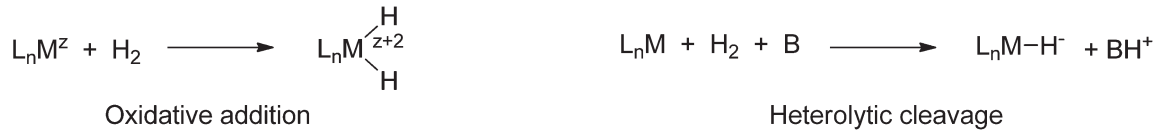

Fig. 1 Two pathways for the activation of dihydrogen.

interaction between a weakly acidic proton (NH or OH) and a transition metal hydride has a substantial strength (3–7 kcal mol^{-1}), which lies in the range observed in conventional hydrogen bonds. Therefore it can influence the structure and reactivity of metal hydride complexes. It has been shown that dihydrogen bonded adducts can be formed prior to proton transfer from HA to a metal hydride to form a dihydrogen complex. This reaction is the reverse of the heterolytic splitting of H_2; thus complexes exhibiting H···H interactions can be considered as intermediates in the activation process.[19,20]

The ancillary ligands (usually phosphines) have an important influence on dihydrogen bond formation. Morris *et al.* compared the strength of intramolecular IrH···H bonds in complexes with PCy_3 and PPh_3. The stronger dihydrogen bond was formed in complexes containing PCy_3, which increases the basicity of the hydride.[21] Crabtree, Eisenstein *et al.*[13a,b] found that while PPh_3 favors the heterolytic splitting of dihydrogen by iridium complexes (assisted by a pendant amino group), more basic alkylphosphines form an η^2–H_2 complex. In our research group, a series of wide bite angle diphosphine ligands has been developed. Much effort has been devoted to the understanding of the influence of diphosphine ligands on the reactivity and catalytic performance of transition metal complexes.[22–24]

On the other hand, pyridylphosphine ligands exhibit a very rich chemistry.[25,26] Owing to the presence of both soft and hard donor atoms, they can stabilize metal ions in several oxidation states and geometries. When they act as chelating ligands they can stabilize a catalyst precursor, while the nitrogen atom de-coordinates easily to provide a vacant site for substrate binding and further reaction. Furthermore, the free pyridyl moiety can act as an intramolecular base to assist the heterolytic cleavage of H_2 as shown by Jalón *et al*. for Ru–H_2 complexes.[27] These characteristics are very important in catalytic cycles, which often involve changes in the oxidation state and the coordination number of the metal centers. The cooperative nature of pendant base containing metal complexes can lead to strongly improved performance in many catalytic reactions.[28] Noyori's catalyst and the Shvo catalyst, both Ru, are examples of such metal–ligand bifunctional catalysts.[29] A simple ligand used as such is a secondary phosphine oxide (SPO) ligand in Pt and Rh complexes.[30] The importance of a base is also illustrated by systems capable of metal free activation of dihydrogen such as carbenes and frustrated Lewis pairs.[31]

We wish to report here the study of the influence of the ancillary ligands on the structure of complexes of the type [M(diphosphine)(2-(diphenylphosphino)pyridine)]$^{2+}$ (M = Pd, Pt) as well as their reactivity towards dihydrogen. The resulting complexes contain both a hydride and a protonated pyridyl moiety in close proximity to one another, which makes them potential candidates for dihydrogen bonding.

Results and discussion

Synthesis of [(diphosphine)M(2-(diphenylphosphino)-pyridine)]$^{2+}$ complexes (1a–d)

Chart 1 shows the diphosphine ligands used for this study, together with their calculated, so-called natural bite angles (β_n), as defined by Casey *et al.*[32,33]

The dicationic platinum and palladium complexes containing a chelating 2-(diphenylphosphino)pyridine (Ph_2PPy) ligand were prepared by reaction of the corresponding (diphosphine)-MCl_2 (M = Pt, Pd) with silver triflate, followed by addition of 2-(diphenylphosphino)pyridine (Scheme 1). When silver triflate is added to a CH_2Cl_2 solution containing the dichloride precursor, a deeply colored solution is formed. After a few minutes precipitation of AgCl is observed. Upon addition of 2-(diphenylphosphino)pyridine, the color changes immediately to yellow for the complexes containing Xantphos-type ligands and orange (Pt) or purple (Pd) for the dppf analogs.

Complexes **1a–d** (Pt and Pd) were characterized in solution by multinuclear NMR spectroscopy. ^{31}P NMR spectroscopic data are summarized in Table 1. In most cases, the spectra of the platinum and palladium complexes are very similar, and they will be described together. The few differences will be discussed afterwards. The $^{31}P\{^1H\}$ NMR spectra display an AMX spin system (Fig. 2) for the *cis* isomer and an A_2X system for the *trans* isomer. For complexes **1a–c** only the *cis* isomer was observed, whereas for complexes **1d** containing the Xantphos ligand, a mixture of the *cis* and *trans* isomers was obtained. The AMX spin system is consistent with a structure in which the diphosphine is coordinated in a *cis* fashion and 2-(diphenylphosphino)pyridine acts as a chelating ligand. Bidentate coordination of 2-(diphenylphosphino)pyridine is

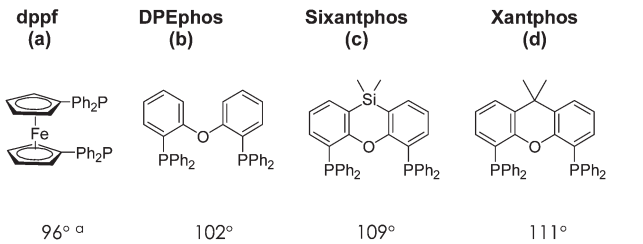

Chart 1 Diphosphine ligands used and natural bite angles in degrees. [a]Value from crystal structure. All values taken from ref. 22.

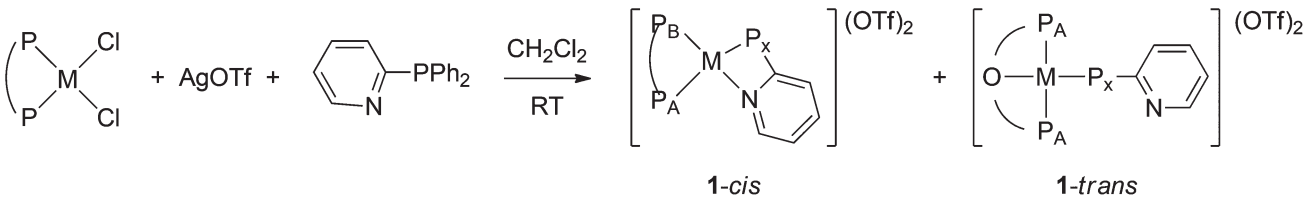

Scheme 1 Synthesis of complexes (Pt, Pd)**1a–d**. Phenyl groups on phosphorus atoms have been omitted for clarity, P = PPh_2.

Table 1 $^{31}P\{^1H\}$ spectroscopic data for complexes **1a–d**

Complex	J_{PA-PM} (Hz)	J_{PA-PX} (Hz)	J_{PM-PX} (Hz)	J_{Pt-PA} (Hz)	J_{Pt-PM} (Hz)	J_{Pt-PX} (Hz)	δ_{PA} (ppm)	δ_{PM} (ppm)	δ_{PX} (ppm)	δ_{Pt} (ppm)
Pt1a	12.0	364	19.5	2737	3496	2058	24.0	9.16	−38.3	−4083
Pt1b	16.3	372	15.8	2829	3536	2143	15.2	−7.5	−39.2	−4063
Pt1c	19.3	360	15.2	2772	3563	2142	12.8	−6.6	−40.1	−4082
Pt1d										
Cis	24.3	358	12.2	2800	365	2118	12.0	−6.5	−41.3	−4073
Trans	—	12.1	—	2503	—	4447	39.2	—	16.3	−3972
Pd1a	8.5	408	14	—	—	—	30.7	41.7	−42.3	—
Pd1b	3.7	412	n.r.[b]	—	—	—	20.5	20.1	−46.1	—
Pd1d[a]										
Cis	4.9	388	n.r.[b]	—	—	—	12.9	18.8	−45.1	—
Trans	—	23.1	—	—	—	—	36.2	—	35.1	—
Pt1a-Me[a]										
I	12	354	21	2728	3533	2075	20.9	5.0	−40.0	n.d.[c]
II	425	15	19	3461	2538	3764	16.4	23.2	15.8	n.d.[c]
Pd1a-Me[a]	n.r.[b]	389.4	12.2	—	—	—	25.1	41.1	−40.8	—

All spectra were measured in CD_2Cl_2 at room temperature unless otherwise stated. [a] At 233 K. [b] Non-resolved. [c] Not determined.

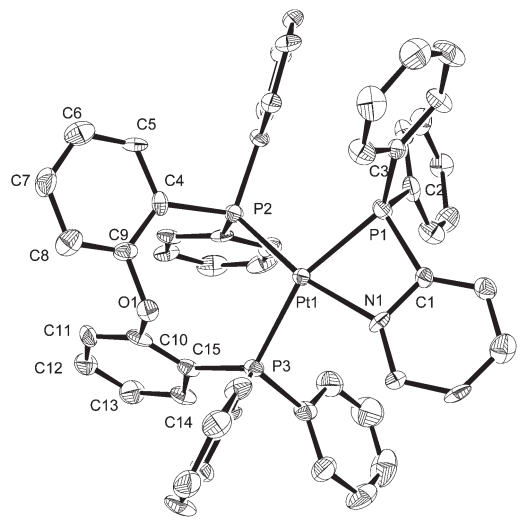

Fig. 2 Molecular structure of $[(\kappa^2\text{-DPEphos})Pt(\kappa^2\text{-}Ph_2PPy)][OTf]_2{\cdot}3(CH_2Cl_2)$ (**Pt1b**). The displacements ellipsoids are drawn at a 50% probability level. The hydrogen atoms, the triflate anions and solvent of crystallization have been omitted for clarity.

confirmed by the large up-field shift of P_X which show resonances between δ = −38 and δ = −46 ppm. In the case of the platinum complexes, the value of the P–Pt coupling constant (≈2000 Hz) is small compared to the values observed for the other two phosphorus nuclei (2500–3500 Hz). Both the chemical shift and the J_{PX-Pt} coupling are characteristic of a strained four-membered ring.[34,35]

The chelating coordination of the 2-(diphenylphosphino)-pyridine is usually also reflected in the ^1H NMR spectrum of the corresponding metal complexes, by a downfield shift of the proton *ortho* to the nitrogen (H_6) in the pyridine moiety. When the pyridine nitrogen coordinates, the resonance of H_6 shifts to higher frequencies compared to the free ligand[36,37] (above δ = 9 ppm for the chelate *vs.* δ = 8.72 ppm for the free ligand in $CDCl_3$). Although for complexes **1a–d** the resonance for H_6 is clearly separated from the rest of the aromatic signals, it appears at a lower value than expected. A similar trend was observed by James and co-workers,[38] who studied ruthenium complexes containing the 2-pyridylphosphines $PPh_{3-x}(Py)_x$ (x = 1–3). Tris-(2-pyridyl)phosphine acted as a tridentate ligand with the phosphorus atom and two of the pyridine nitrogens coordinated to ruthenium. They observed that the signals for H_6 in the coordinated pyridyl rings appeared down-field compared to the resonance of H_6 in the non-coordinated pyridine. This may be due to the proximity of the phenyl groups of the diphosphines to the pyridyl ring, causing an unusual shielding of H_6. As will be discussed later, the phenyl groups of wide bite angle diphosphines tend to embrace the metal ion and cause important steric interactions with the other coordinated ligands.

Although the purple color of **Pd1a** might suggest a Pd–Fe bond,[39] no NMR or UV spectroscopic evidence for such an interaction was found. Indeed, both the ^{31}P and the ^1H spectra are very similar for the platinum and palladium complexes.

The ^{31}P spectrum of **Pt1d** displays a triplet (P_A) and a doublet (P_X) with an intensity ratio of 2 : 1, in addition to the

AMX system described above. These signals correspond to the *trans* isomer of **Pt1d**, in which 2-(diphenylphosphino)pyridine acts as a monodentate ligand (Scheme 1). For compound *trans*-**Pt1d**, the phosphorus atom of the 2-(diphenylphosphino)pyridine ligand (P_X) displays a very large Pt–P coupling constant of J_{PX-Pt} = 4447 Hz. This value is commonly observed for phosphorus atoms *trans* to oxygen donor ligands.[40] Furthermore, while the chemical shift of the ^{195}Pt nuclei in all *cis* complexes does not vary by more than 20 ppm, δ_{Pt} of *trans*-**1d** is about 100 ppm higher than the average value of the former complexes (Table 1), indicating that there is an important difference in the environment of the platinum nucleus in *cis* and *trans*-**Pt1d**. This points to an interaction between the platinum center and the oxygen of the Xantphos backbone, indicating that Xantphos coordinates as a tridentate ligand. This *mer*-P,O,P-κ^3 type of coordination for Xantphos has been observed in cationic Rh(I) and Pd(II) complexes. It has been suggested that the metal–oxygen interaction can stabilize the *trans* isomer with respect to the *cis* one in which this interaction is not present.[41–44] For Xantphos and DPEphos both *mer*-κ^3-P,O,P and *fac*-κ^3-P,O,P coordinations have been observed recently and this flexibility played an important role in the catalytic reactivity of the complexes in hydroacylation.[45,46] The *mer*-κ^3-P,O,P coordination of Xantphos for Pt was confirmed by single crystal X-ray diffraction, which will be discussed later.

The ^{1}H NMR spectrum of complex **Pt1d** displays two signals for the methyl groups in the backbone at δ = 1.77 and δ = 1.82 ppm. Integration of these signals indicates that the *cis* and *trans* isomers are present in a 1 : 1 ratio. For complex **1c**, which exists as the *cis* isomer only, one signal (δ = 0.78 ppm) was observed for the CH_3 groups in the backbone.

The corresponding palladium complex [(Xantphos)Pd(PPy)](OTf)$_2$ (**Pd1d**) shows fluxional behavior. The ^{31}P NMR spectrum displays only a broad singlet for the Xantphos ligand at room temperature, while the ^{1}H NMR spectrum shows a slightly broad singlet for all methyl groups and broad signals for the aromatic protons. At low temperature, the singlet in the ^{31}P NMR spectrum becomes less intense and other signals start to emerge from the base line. At 233 K two sets of signals can be distinguished in the ^{31}P NMR spectrum: a doublet and a broad triplet with an intensity ratio of 2 : 1 (major product), and an AMX spin system (minor product) similar to that described above for complexes **1a–b**. As discussed above, the two sets of resonances correspond to the *cis* and *trans* isomers of **Pd1d** (Scheme 1). Thus the AMX spin system was assigned to the *cis* isomer containing chelating 2-(diphenylphosphino)-pyridine. The second set of resonances corresponds to the *trans* isomer, in which Xantphos coordinates in a tridentate *mer*-κ^3-P,O,P fashion.[35,43] In the ^{1}H NMR spectrum at 233 K three signals are observed for the methyl groups in the ligand backbone, two of equal intensity for the *cis* isomer (δ = 1.9 and δ = 1.6 ppm) and one (δ = 1.7 ppm) for the *trans* isomer. Integration of these signals shows a *trans* : *cis* ratio of 2.5, which was confirmed by integration of the ^{31}P spectrum. At 193 K, the *trans* : *cis* ratio is 1.3, indicating that the formation of the pyridylphosphine chelate is favored at low temperature. For the analogous platinum complex (**Pt1d**), neither exchange between the *cis* and *trans* isomers was observed at room temperature, nor did the ratio between the two isomers change with temperature.

Analogs of complexes **1a** using the bulkier ligand diphenyl-2-(6-methyl-pyridyl)phosphine (**Pt1a-Me** and **Pd1a-Me**) were prepared following the same methodology as for **1a–d**. Both platinum and palladium complexes **1a-Me** gave rise to very broad signals at room temperature. Nevertheless, a different fluxional behavior is observed for **Pt1aMe** and **Pd1aMe**. In the case of platinum, two complexes can be observed upon lowering the temperature. At 233 K, two distinct sets of signals were observed in the ^{31}P NMR spectrum in a 1 : 1 ratio. The first set corresponds to a complex analogous to **Pt1a** in which 2-(diphenylphosphino)pyridine coordinates in a chelating fashion, *cis*-κ^2-P,N. Thus, its spectroscopic properties are very similar to those described for **Pt1a** (Table 1).

The second set of signals is an ABX spin system for which both the chemical shifts and the P–Pt coupling constants indicate that 2-(diphenylphosphino)pyridine acts as a κ^1-P monodentate ligand. The ABX spin system rules out a *trans* structure similar to *trans*-**1d** or a dimeric structure. The ^{1}H NMR spectra show two signals (δ = 1.59 and δ = 2.40 ppm) for the methyl groups of the pyridyl moiety, and a total of seven signals for the Cp protons in the dppf ligand. Two of the signals (4 protons in total) appear at δ = 3.26 and δ = 3.23 ppm and are shifted up-field by more than 1 ppm, as observed for **1a**. The remaining signals (integrating for 12 protons) appear between δ = 5.09 and δ = 4.27 ppm. This indicates that in both products dppf is coordinated in a *cis* fashion (Scheme 2).

In the second product (**Pt1aMe-II**), 6-methyl-2-(diphenylphosphino)pyridine is not chelating and the fourth coordination position is probably occupied by the triflate anion. The IR spectrum shows two split bands for $\nu(SO_3)$ at 1260 and 1005 cm^{-1}. These bands have been previously assigned to mono-coordinated sulfonates.[47] Although triflates are known to be weakly coordinating anions, the IR data and the fact that the microanalysis of a sample containing both products is correct show that both compounds have the same composition (see the Experimental section). The broad spectra observed at room temperature indicate exchange between the two species.

In the case of palladium, complex **Pd1a-Me** shows fluxional behaviour at room temperature. The ^{31}P NMR spectrum reveals an exchange process between the two phosphorus nuclei of dppf. The extra steric bulk introduced by the methyl group induces a facile de-coordination of the pyridyl moiety,

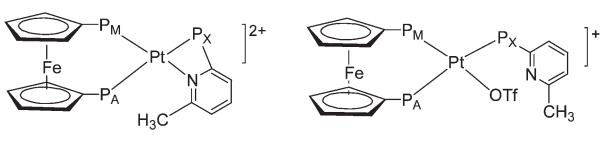

Pt1aMe-I Pt1aMe-II

Scheme 2 Platinum complexes formed when 6-methyl-2-(diphenylphosphino) pyridine is used.

probably assisted by the counterion or traces of free phosphine in solution. Rotation in the five-coordinated species has a low barrier and results in exchange of the positions of P_A and P_M. Upon lowering the temperature all signals broaden further, but at 253 K they start to re-emerge from the base line. At 193 K the ^{31}P NMR spectra show a well resolved AMX pattern corresponding to [(dppf)Pd(κ^2-6-methyl-2-(diphenylphosphino)-pyridine)](OTf)$_2$, indicating that the dissociation or the isomerization of the square planar complex is slow on the NMR timescale at this temperature.

A second species can be observed in the ^{31}P NMR spectrum of **Pd1a-Me** at room temperature. It displays a doublet at −14.9 ppm and a triplet at 42.3 ppm, with a coupling constant of 13.4 Hz. The chemical shifts and the coupling constant are very similar to those reported by Sato *et al.* for [(η^3-dppf)-Pd(PPh$_3$)](BF$_4$)$_2$, which involves an Fe–Pd dative bond.[39] Therefore we propose that the second species in solution is [(κ^3-P,Fe,P-dppf)Pd(κ^1-6-methyl-2-(diphenylphosphino)pyridine)](OTf)$_2$. This product is not involved in the exchange process mentioned above, so it displays sharp NMR signals at room temperature. At 193 K, the signals for this product represent less than 5% of the total intensity. Remarkably, **Pd1a-Me** displays a very different behavior from its platinum counterpart. For the Pt complex, the species containing a chelating 6-methyl-2-(diphenylphosphino)pyridine [(dppf)Pt(κ^2-6-methyl-2-(diphenylphosphino)pyridine)](OTf)$_2$ and the one in which the coordinated pyridyl has been replaced by the anion do not exchange on the NMR time scale and separate sets of signals for each isomer are observed. Furthermore, a complex with an Fe–Pt bond was not detected at any temperature.

Solid state structures

The platinum complexes **Pt1b**, **Pt1c** and **Pt1d** were further characterized by single crystal X-ray diffraction. Suitable crystals were grown by slow diffusion of diethyl ether or hexanes into dichloromethane solutions of the corresponding complex.

Selected bond distances and angles are presented in Table 2. The structures found in the solid state are in agreement with those proposed in solution from the NMR data discussed above. Thus, complexes with DPEphos (**b**) and Sixantphos (**c**) form *cis* complexes, while for Xantphos (**d**) both *cis* and *trans* isomers are present in solution. In the latter case, only the *trans* isomer could be crystallized. The X-ray structure of *trans* **Pt1d** confirms the P,O,P coordination mode of Xantphos, which was proposed based on the J_{Pt-Px} coupling constant and the ^{195}Pt chemical shift. The solid state structures of **Pt1b** and **Pt1c** show that there is considerable interaction between the phenyl groups of the diphosphine ligand and those of 2-(diphenylphosphino)pyridine. This interaction becomes more important as the bite angle increases. In the case of the Xantphos ligand 2-(diphenylphosphino)pyridine is forced to act as a monodentate ligand. The "embracing effect" of the phenyl rings in wide bite angle diphosphines in palladium allyl complexes was studied by van Haaren *et al.*[48]

Table 2 Selected bond distances (Å) and bond angles (°) for complexes **Pt1b–d**

	DPEphos (**1b**)	Sixantphos (**1c**)	Xantphos (**1d**)
Pt–P1	2.324(3)	2.3011(14)	2.2387(7)
Pt–P2	2.279(3)	2.2638(13)	2.3171(5)
Pt–P3	2.337(3)	2.3852(13)	2.2976(5)
Pt–O1	3.488(9)	2.725(3)	2.1889(18)
Pt–N1	2.112(8)	2.109(4)	—
P1–C1	1.804(13)	1.818(5)	1.833(2)
∠P1–Pt–P2	99.32(10)	99.42(5)	96.90(2)
∠P2–Pt–P3	98.96(10)	94.95(5)	162.22(2)
∠P3–Pt–N1	92.3(3)	96.50(11)	—
∠P1–Pt–N1	68.9(3)	69.08(11)	—
∠P2–Pt–N1	168.1(3)	168.49(11)	—
∠P1–Pt–P3	157.29(10)	164.89(5)	100.22(2)
∠Pt–P1–C1	83.3(4)	83.35(16)	110.78(11)
∠P1–C1–N1	103.6(7)	103.4(3)	—
∠P2–Pt–O1	—	—	80.97(4)
∠P3–Pt–O1	—	—	82.37(4)
∠P1–Pt–O1	—	—	174.69(4)

For complexes **Pt1b** and **Pt1c** the coordination sphere of the platinum atom consists of a *cis* coordinated diphosphine ligand and chelating 2-(diphenylphosphino)pyridine. As commonly observed in complexes containing a chelating pyridylphosphine, the bond angles involving the four-membered Pt1–N1–C1–P1 ring show an important deviation from the ideal 90° value. The P1–Pt–N1 angles of 68.9(3)° for **Pt1b** and 69.08(11)° for **Pt1c** are slightly smaller than those reported for other platinum complexes (70.8(5)° for [PtCl(κ^2-Ph$_2$PPy)-(PPh$_2$PPy)]$^+$[49] and 70.4(5)° in [PtMe(κ^2-Ph$_2$PPy)(PPh$_2$PPy)]$^+$).[50]

The smaller bite angle of the 2-(diphenylphosphino)pyridine ligand may be due to steric bulk of the diphosphine, compared to the smaller methyl and chloride ligands. The intrachelate angles of P1–C1–N1 (103.6(7)° in **Pt1b** and 103.4(3)° in **Pt1c**) and Pt–P1–C1 (83.3(4)° and 83.35(16)°, respectively) show the same deviation from the ideal values as observed in the above-mentioned complexes.

The Pt–N1 distance in **Pt1b/c** is almost 0.1 Å longer than the one reported by Jain *et al.*[50] and Farr *et al.*[49] in the above-mentioned platinum complexes, but in the same range as those observed in [Ru(κ^2-Ph$_2$PPy)(CO)$_2$Cl$_2$][51] and [PdCl(κ^2-Me$_2$PPy)(PMe$_2$PPy)]$^+$.[52]

The platinum atom in **Pt1b** is shifted 0.124 Å away from the least-squares plane determined by itself, the three phosphorus atoms and the nitrogen atom, while the deviation is only 0.043 Å in **Pt1c**. Especially for the complex **1b** (DPEphos), the deviation from the coordination plane is much larger than the 0.017 Å or the 0.026 Å observed in [PtMe(κ^2-Ph$_2$Ppy)(Ph$_2$PPy)]-[BPh$_4$][50] and [Ru(η^2-Ph$_2$PPy)(CO)$_2$Cl$_2$][51] respectively. The larger deviation from the coordination plane may be due to the presence of the additional chelating ligand, while in the two other complexes reported the additional ligands are monodentate and therefore can coordinate at an angle near the ideal 90° value. Because DPEphos (**b**) and Sixantphos (**c**) have natural bite angles larger than 100°, they will force a geometry with a more open P2–Pt–P3 angle which leads to further distortion around the Pt center. In fact, the P2–Pt–P3 angle is smaller

(98.96(10)° in **Pt1b** and 94.95(5)° for **Pt1c**) than expected from these wide bite angle diphosphines. Particularly for the Sixantphos complex (**1c**), the value of 94.95(5)° is at the lower end of the flexibility range for this ligand (93–130°).[53] In complex **Pt1b** the P2–Pt–P3 angle is slightly smaller than the P–Pd–P angle observed in palladium complexes containing DPEphos prepared in our group (from 100.82° to 103.93°).[54,55] Again, the smaller bite angle may be caused by the steric interaction between the phenyl rings of the diphosphine and those on 2-(diphenylphosphino)pyridine (Fig. 2 and 3).

The backbone of the DPEphos ligand is highly bent (Fig. 2), the planes containing the aromatic rings form an angle of 102.9°. This conformation has been observed in other square planar complexes of DPEphos.[54,55] In the case of complex **Pt1c** (Fig. 3), one of the aromatic rings of the Sixantphos backbone is bent to the back, the angle between the planes formed by (C4 to C9) and (C10 to C15) is 40.2°.

The Pt–O distance in **Pt1b** is 3.488(9) Å, but it is considerably shorter in **Pt1c** (2.725(3) Å). The latter distance is only slightly longer than the 2.714(3) Å reported for [Sixantphos-Pd(4-C_6H_4CN)Br][54] in which the diphosphine ligand adopts a *trans* geometry, and thus forces the oxygen atom close to the metal. This is, to a lesser extent, also the case in **Pt1c**. Because of the rigidity of Sixantphos, the Pt–O bond cannot be much longer. A weak platinum–oxygen bond was proposed in a Pt(II)–β-diketonato complex in which the Pt–O distance was 2.796(6) Å.[56] Similar Pd–O distances have been reported in five-coordinated palladium(II) complexes[57,58] and thus the short distance observed in **Pt1c** might also indicate the presence of a weak Pt–O interaction.

In complex **Pt1d** (Fig. 4), Xantphos acts as a tridentate ligand. The Pt–O distance is 2.1889(18) Å, which is slightly shorter than the 2.1537(14) Å observed in [*mer*-κ^3-Xantphos-Pd(4-C_6H_4CN)]$^+$.[54] This is probably caused by the larger *trans* influence of the aryl ligand compared to the phosphine in **1d**. The geometry around the metal is square planar. Because of the rigidity of the Xantphos ligand, P2 and P3 are bent down from the coordination plane and the P2–Pt–P3 angle is 162.22(2)°. The O–Pt–P1 angle (174.69(4)°) is closer to the ideal value of 180°. The Xantphos backbone is also bent, the angle between the aromatic rings (C4 to C9) and (O1, C9 to C12) is 8.3°, while the angle between the latter and the (C11 to C16) plane is 10.6°. The Pt–P2 and Pt–P3 distances are similar to those observed in other *trans* coordinated Pt(II) complexes.[59] The Pt–P1 bond length in **Pt1d** (2.2387(7) Å) is similar to those observed in platinum complexes in which 2-(diphenylphosphino)pyridine acts as a P-monodentate.[49,50] This bond is also considerably shorter than those in **Pt1b/c**.

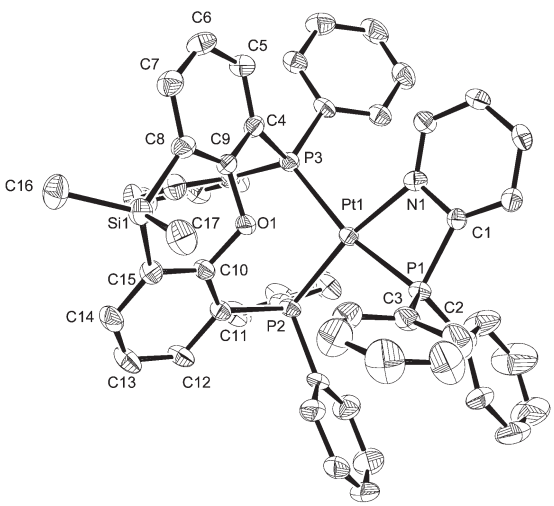

Fig. 3 Molecular structure of [(*cis*-κ^2-Sixantphos)Pt(κ^2-Ph_2PPy)][OTf]$_2$·CH_2Cl_2 (**Pt1c**). The displacement ellipsoids are drawn at a 50% probability level. The hydrogen atoms, the triflate anions and solvent of crystallization have been omitted for clarity.

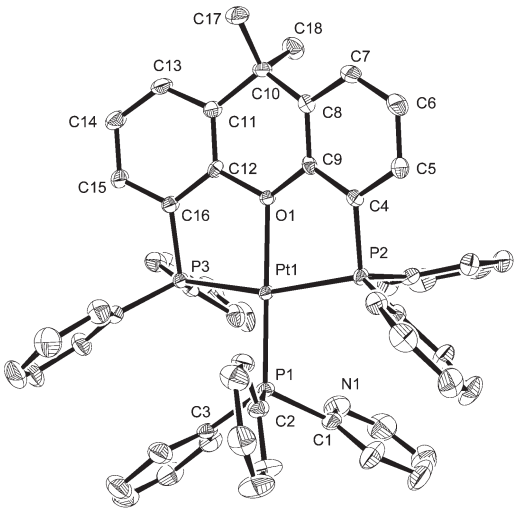

Fig. 4 Molecular structure of [(*mer*-κ^3-Xantphos)Pt(κ^1-P-Ph_2PPy)][OTf]$_2$·0.5(H_2O) (*trans***1d**). The displacement ellipsoids are drawn at a 50% probability level. The hydrogen atoms, the triflate anions and solvent of crystallization have been omitted for clarity.

Two factors play an important role in the coordination chemistry of **Pt1a–d**; the natural bite angle of the diphosphine ligands, and the steric constraints imposed by the chelation of 2-(diphenylphosphino)pyridine. While dppf and DPEphos can easily coordinate in a *cis* fashion, the bite angle of Sixantphos and particularly of Xantphos is too large for the ideal 90° P–M–P angle in a *cis* coordinated square planar complex, but neither of them is large enough for ideal *trans* coordination. In fact, the crystal structure of **Pt1d**, as well as the other reported structures with a *trans* coordinated Xantphos ligand, shows that the P–M–P angle is always less than 165° with the phosphorus atoms bent away from the plane. Diphosphines with a wide bite angle also have a large cone angle, which results in less free space around the metal center for coordination of other ligands. As the chelation of 2-(diphenylphosphino)pyridine increases the steric bulk around the metal center, bidentate coordination of 2-(diphenylphosphino)pyridine becomes less favoured as the bite angle increases. Furthermore, chelation of 2-(diphenylphosphino)pyridine is unfavourable by the intrinsic strain of the four-membered ring. Nevertheless,

2-(diphenylphosphino)pyridine acts as a chelating ligand in **Pt1a–d**. Obviously, the Pt–N bond is strong enough to stabilize the highly strained geometries in **Pt1a–c**, especially in the case of **Pt1c** in which the Sixantphos ligand is forced to adopt an uncommonly small bite angle. When the steric hindrance in **Pt1d** becomes more important, chelation of the 2-(diphenylphosphino)pyridine is more difficult, and a mixture of *cis* and *trans* **Pt1d** is formed. Thus, the structure of complexes **1a–d** is a compromise between the steric hindrance induced by the bite angle of the diphosphine and the stabilization due to the chelation of the 2-(diphenylphosphino)pyridine.

Heterolytic activation of H_2

Although the activation of dihydrogen by platinum and palladium complexes and the formation of the respective metal hydrides have been proposed to play an important role in the mechanism of the palladium catalyzed hydroformylation[60,61] and hydrogenation[62] the number of hydride complexes which have been prepared and isolated by this route[63] is still limited. Both Pt and Pd complexes with 2-(diphenylphosphino)pyridine and ligands **a–d** were tested for their reactivity toward dihydrogen.

Platinum complexes. Complexes **Pt1b–d** react with dihydrogen under mild conditions (4 bar, 40 °C, 16 h) to afford cationic platinum hydrides **2b–d** according to Scheme 3.

In this reaction, the coordinated pyridine moiety acts as a hemilabile ligand to provide a vacant coordination site as well as an internal base to assist the heterolytic splitting of the dihydrogen molecule.[27] The new hydride complexes were characterized by multinuclear NMR spectroscopy. The ^{1}H and ^{31}P NMR data are presented in Tables 3 and 4, respectively. The ^{1}H NMR spectrum of **Pt2b–d** shows a characteristic hydride signal between $\delta = -5$ and $\delta = -8$ ppm. The shape of the signal depends on the ligand used. For complexes **Pt2b** and **Pt2c** containing DPEphos and Sixantphos respectively, all the H–P couplings are resolved and the hydride signal appears as a doublet of doublets of doublets, with the corresponding Pt satellites. For complex **Pt2d** (Xantphos), the two *cis* H–P coupling constants are not well resolved, the hydride signal appears as a slightly broad doublet of triplets, with Pt satellites. Protonation of the pyridine moiety was confirmed by the broad signal at about 15 ppm, with an integration ratio with the hydride of 1 : 1. This signal broadens and shifts slightly to higher fields on lowering the temperature.

The new complexes show an ABX spin system in the ^{31}P NMR spectrum, in which the AB part is formed by the two phosphines *trans* to one another and P_X corresponds to the phosphorus *trans* to the hydride ligand. This assignment is confirmed by the relatively small P_X–Pt coupling constant ($J_{PX-Pt} \approx 2200$ Hz), which is normally observed for nuclei *trans* to hydrides. At the same time, the increase of more than 1000 Hz of the P_B–Pt coupling constant indicates a release of the ring strain. Complete spectroscopic data are shown in Tables 3 and 4. The ^{1}H and ^{31}P spectra did not change significantly on lowering the temperature, apart from some broadening of the signals below 233 K. At 203 K, the N–H proton is no longer observed.

Surprisingly, complex **Pt1a** with the dppf ligand did not react with dihydrogen, not even at 10 bar and 50 °C. The use of a more basic solvent such as acetone led to complete decomposition of the starting material without formation of the desired hydride product. When one equivalent of an external base (Et_2NH or DIPEA) was used, a hydride complex was formed together with the salt of the amine under the same reaction conditions as for **Pt1b–d**. This complex could be protonated afterwards with HOTf to afford **2a**, in which the pyridine moiety is protonated. Although the bite angle and the basicity of dppf are similar to those of DPEphos, **Pt1a** and **Pt1b** show a strikingly different reactivity towards the heterolytic activation of dihydrogen. More information on the

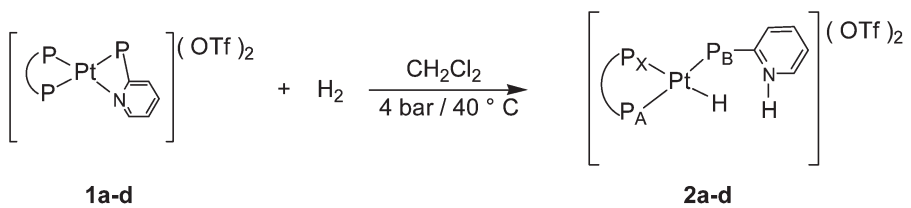

1a-d **2a-d**

Scheme 3 Reaction of complexes **Pt1b–d** with dihydrogen. P = PPh_2.

Table 3 $^{1}H\{^{31}P\}$ NMR data for the hydride complexes **Pt2a–d**

Complex	Ligand	δ_H (ppm)	δ_{N-H} (ppm)	J_{PA-H} (Hz)	J_{PB-H} (Hz)	J_{Px-H} (Hz)	J_{Pt-H} (Hz)
Pt2a	Dppf	−5.72	15.1	11.7	18.5	154	762
Pt2a-Me[a] *cis*		−5.61	14.35	10.5	22.5	150	750
Pt2a-Me[a] *trans*		−5.11		13.5	—	162	797
Pt2b	DPEphos	−6.81	14.9	13.0	16.5	163	739
Pt2c	Sixantphos	−7.53	15.1	13.7	14.7	158	732
Pt2d	Xantphos	−8.14	15.3	14.4	n.r [b]	158.9	714

NMR spectra were measured at 300 MHz in CD_2Cl_2 at room temperature, unless otherwise stated. [a] At 233 K. [b] not resolved.

Table 4 $^{31}P\{^1H\}$ NMR spectroscopic data for the hydride complexes **Pt2a–d**

Complex	J_{PA-PB} (Hz)	J_{PA-PX} (Hz)	J_{PB-PX} (Hz)	J_{Pt-PA} (Hz)	J_{Pt-PB} (Hz)	J_{Pt-PX} (Hz)	δ_{PA} (ppm)	δ_{PB} (ppm)	δ_{PX} (ppm)
Pt2a [b]	364	10.81	−8.8	3033	2755	2310	28.7	21.8	22.9
Pt2a-Me[a] *cis*	372	18.2	−21.9	2750	3079	2395	29.9	20.7	23.6
Pt2a-Me[a] *trans*	—	19.4	—	2863	—	2255	25.3	—	22.9
Pt2b[b]	360	31.7	−10.5	2905	2944	2217	23.4	16.4	16.5
Pt2c[b]	370	12.7	−24.3	3030	2922	2286	23.8	20.1	15.8
Pt2d[b,c]	375	16.3	−19.6	3045	2937	2298	23.0	17.7	15.8

All spectra were measured at 121.5 MHz in CD_2Cl_2 at room temperature, unless otherwise stated. [a] At 233 K. [b] Chemical shifts and coupling constants calculated with gNMR. [c] At 160.5 MHz.

electronic properties of the metal center was sought by means of ^{195}Pt NMR. The chemical shift of ^{195}Pt nuclei is sensitive to the ligands present in the coordination sphere and is therefore a useful probe of the electronic environment of the metal.[64,65] Nevertheless, as can be seen in Table 1, the ^{195}Pt chemical shifts for complexes **Pt1a** and **Pt1b** are not significantly different, indicating that there are no large differences in the coordination environment of these two complexes.

The explanation for the different reactivity of **Pt1a** compared to **Pt1b** may lie in the smaller cone angle of dppf (229.7°) compared to that of DPEphos (240.2°).[54] For allylic alkylation reactions van Haaren *et al.* observed an important difference in the activity and selectivity of the palladium catalysts with dppf compared to the one with DPEphos.[48] In the case of **Pt1b–d**, the steric interaction between the phenyl groups of the Xantphos-type ligands with 2-(diphenylphosphino)pyridine may labilize the Pt–N bond, whereas in **Pt1a** the stronger coordination of the pyridyl moiety results in lack of reactivity. The driving force for the formation of the hydride complexes is probably the release of the ring strain in 2-(diphenylphosphino)pyridine. Indeed, when the latter ligand was replaced by 3-(diphenylphosphinomethyl)pyridine, which forms a 6-membered metallacycle, the reaction with dihydrogen was very slow. The built-in base in complexes **Pt1b–d** does not accelerate the reaction. The reaction of $[(DPEphos)Pt(PPh_3)](OTf)_2$ with dihydrogen and one equivalent of an external base (DIPEA) is as fast as the reaction of complex **Pt1b**. This indicates that either the rate of de-coordination of the pyridyl moiety is the rate-limiting step or that the equilibrium concentration of the tricoordinate species is too low to lead to an appreciable rate of H_2 cleavage.

Complex **Pt1a-Me** (*cis* and *trans*) did react under the same conditions as **Pt1b–d** to give a mixture of two hydride species. The reaction mixture displays very broad signals in the ^{1}H and the ^{31}P NMR spectra at room temperature. On lowering the temperature to 233 K relatively sharp multiplets appeared and it was possible to identify three sets of peaks. One set corresponds to unreacted starting material (**Pt1a-Me-I**) which is present in about 10%. The second set of signals corresponds to the major species in solution and it is characterized by a doublet of doublets at $\delta = -5.61$ ppm in the ^{1}H NMR spectrum and an ABX spin system in the ^{31}P NMR spectrum. The splitting pattern, coupling constants and chemical shifts are similar to those observed for complexes **Pt2a–d** and therefore

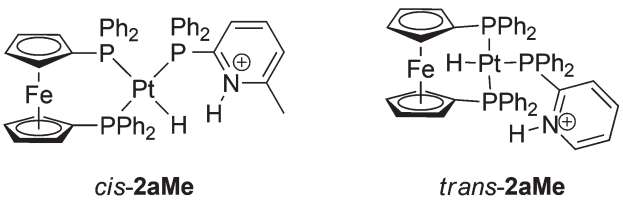

cis-**2aMe** *trans*-**2aMe**

Scheme 4 Products formed from the reaction of **Pt2a-Me** with dihydrogen.

this species was assigned to a hydride *cis*[dppfPtH{2-(6-CH_3-C_5H_3NH)PPh_2}]$^{2+}$ (*cis* **2a-Me**, Scheme 4). Protonation of the pyridine moiety was confirmed by a broad peak at 14.3 ppm. When the solution containing this mixture was filtered over celite, the peaks for *cis* **Pt2a-Me** disappeared almost completely, which enabled the identification of the third product. The ^{1}H NMR spectrum of this product displays a sharp doublet of triplets at $\delta = -5.11$ ppm, while the ^{31}P NMR spectrum shows a doublet and a triplet coupled to one another. The relative intensity of these signals is 2 : 1. Apart from the hydride peaks, the ^{1}H NMR spectrum shows also a signal at $\delta = 2.1$ ppm for the CH_3 of the diphenyl-2-(6-methyl-pyridyl)phosphine ligand and several signals between 4.5 and 3.5 ppm for the Cp protons in dppf, confirming the presence of these two ligands in the product. From these data the third product was assigned to an isomer of **Pt2a-Me** in which dppf is coordinated in a *trans* fashion while 6-methyl-2-(diphenylphosphino)pyridine is *trans* to the hydride (Scheme 4).

Palladium. It is well known that palladium hydrides are generally less stable than their platinum analogues.[66] Therefore, the reaction of the palladium complexes **Pd1a–d** towards dihydrogen was investigated by NMR experiments at low temperature and elevated pressure. As expected, the reaction of the palladium complexes with dihydrogen was much faster than those of the platinum complexes. When the bright orange solution containing [XantphosPd(κ^2-2-(diphenylphosphino)pyridine)]$(OTf)_2$ (**Pd1d**) was pressurized with 4 bar of H_2 at room temperature, the solution became immediately dark brown and extensive precipitation of the palladium metal was observed. Nevertheless almost no change was observed in the ^{1}H and ^{31}P NMR spectra. The tube was subsequently heated to 40 °C and after one hour the peaks of the starting material had completely disappeared. Several multiplets were observed in the ^{31}P NMR spectrum, but no hydride signal could be detected. In order to avoid formation of the palladium metal

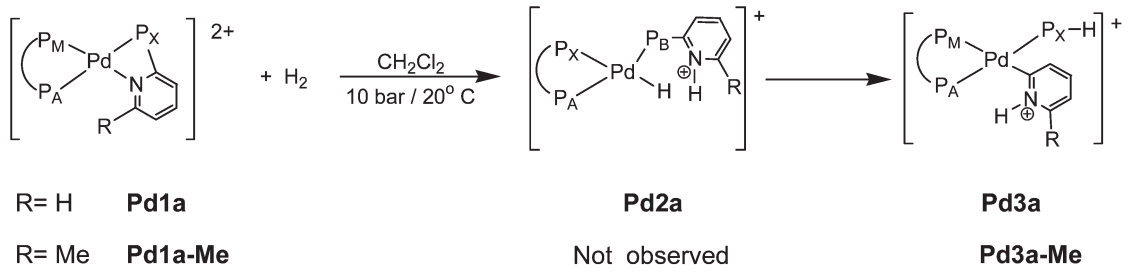

Scheme 5 Reaction of complexes **Pd1a** and **Pd1a-Me** towards dihydrogen. The phenyl groups on the phosphorus have been omitted for clarity (P = PPh_2).

and the associated side reactions, the reaction was performed at low temperature. The solution in the high pressure NMR tube was cooled to −60 °C before pressurizing with 4 bar of dihydrogen, and indeed neither precipitation nor color change was observed. The tube was then introduced into the pre-cooled NMR probe at 213 K. No change in the spectra was observed, even when the solution was warmed to 273 K. After increasing the pressure to 10 bar the reaction was followed at 253 K during 20 hours, but only after 15 hours various small new peaks could be observed. The solution was stored at room temperature for 24 hours and the NMR spectra were measured again at 253 K. [*cis*-κ^2-P,P-XantphosPd(κ^2-2-(diphenylphosphino)pyridine)][OTf]$_2$ (**Pd1d**) remained the main species in solution, but the ^{1}H NMR spectrum showed very small peaks in the hydride region (δ = −9.1 ppm), together with several broad peaks between δ = 13 and δ = 15 ppm. After a total time of 60 hours the starting material was still the major product, but the hydride signal could no longer be observed and several new peaks appeared in the ^{31}P NMR spectrum, which resembled that of the reaction carried out at 40 °C. Although it was not possible to assign all peaks in the ^{31}P NMR spectrum, the observation of multiplets at δ = 220 ppm points towards the formation of phosphido bridged dimers. These dimers are formed as a result of P–C bond cleavage in 2-(diphenylphosphino)pyridine (see below). Similar results were obtained from the reaction of [*cis*-κ^2-P,P-DPEphosPd(κ^2-2-(diphenylphosphino)pyridine)](OTf)$_2$ with dihydrogen, but in this case extensive decomposition can already be observed after 14 hours at room temperature. Apparently, complexes **1d** and **1b** are unable to react with dihydrogen below room temperature, but above this temperature the hydride product reacts further forming unidentified products.

Different reactivity was observed for complexes **Pd1a** and **Pd1a-Me** bearing the dppf ligand. For **Pd1a** no reaction at all was observed under 4 bar of dihydrogen over a period of 8 hours. After 24 hours at 10 bar of H_2 about 30% conversion to a hydride containing product was observed. The high field region of the ^{1}H NMR spectrum shows a broad doublet of doublets at δ = −6.7 ppm, which resolves into a doublet of doublets of doublets upon cooling to 233 K. Four new signals for the Cp protons of dppf were observed between δ = 3.5 and δ = 5 ppm. A broad signal at 15.1 ppm was assigned to the protonated pyridyl moiety. The ^{31}P NMR spectrum shows signals for the starting material together with a new triplet and a doublet of doublets (δ = 22.63 and 32.22 ppm respectively).

These signals were assigned to the new palladium hydride [(dppf)PdH(2-(diphenylphosphino)pyridinium)][OTf]$_2$ **Pd2a** (Scheme 5). Complete conversion to **Pd2a** can be obtained by carrying out the reaction in an autoclave under 10 bar of dihydrogen for 65 hours.

In contrast to this very slow reaction, complex **Pd1a-Me** reacts immediately under 3 bar of dihydrogen at room temperature. The initial dark brown solution turns bright red within 15 minutes and small amounts of palladium metal are formed. Reduction to metallic palladium is avoided if the reaction is carried out at 0 °C. The ^{1}H and ^{31}P NMR spectra showed no starting material remaining. A small hydride signal could be observed in the ^{1}H NMR spectrum, but its intensity was very small compared with the CH_3 and Cp protons, indicating that the main product does not contain a hydride ligand. The ^{31}P{^{1}H} NMR spectrum displays an AMX splitting pattern, similar to that of **Pd1a**, but the disappearance of the signal at δ = −43.6 ppm indicates that 2-(diphenylphosphino)-pyridine is acting as a monodentate ligand. The proton-coupled ^{31}P NMR spectrum reveals a strong P–H coupling in the same range as the *trans* P–P coupling, giving rise to a pseudo-triplet. The ^{1}H NMR spectrum shows a doublet of doublet of doublets centered at δ = 6.1 ppm, which becomes a singlet upon phosphorus decoupling (Fig. 5). The P–H coupling constant (360 Hz) points to the presence of a direct P–H bond. Furthermore, this product displays seven signals for the Cp rings of dppf and a broad singlet at δ = 12 ppm in the ^{1}H NMR spectrum. The ^{13}C{^{1}H}{^{31}P} NMR spectrum displays a singlet at δ = 179.5 ppm which splits into a doublet of triplets when the spectrum is measured phosphorus-coupled (Fig. 5). The values of the carbon–phosphorus coupling constants (J_{CP} = 125 (d) and 12.6 (pt) Hz) indicate that an aryl group is coordinated to the palladium atom. After further characterization by appropriate ^{1}H–^{1}H, ^{1}H–^{31}P and ^{1}H–^{13}C HMQC correlation experiments, **Pd3a-Me** was identified as a palladium-aryl complex arising from the cleavage of the phosphorus–pyridyl bond in coordinated 6-methyl-2-(diphenylphosphino)pyridine (Schemes 5 and 6). Protonation of the nitrogen was confirmed by the broad singlet at δ = 12.2 ppm, which shows a long-range correlation with the protons of the methyl group. Related iridium pyridyl complexes were reported by Carmona *et al.*

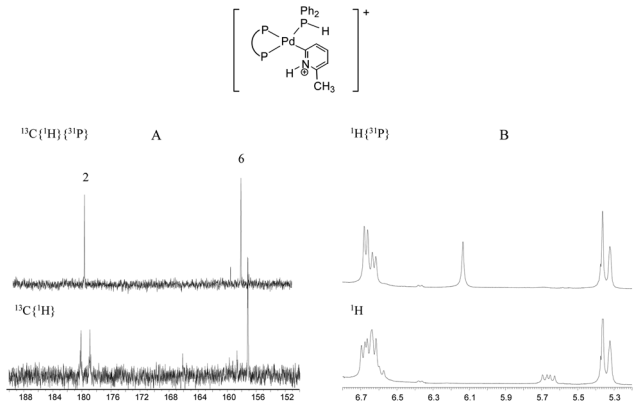

Fig. 5 (A) Section of the ^{13}C NMR spectrum showing the phosphorus coupling on the 2 and 6 carbon atoms of the pyridyl moiety in **Pd3a-Me**. (B) ^1H NMR spectra showing the P–H proton.

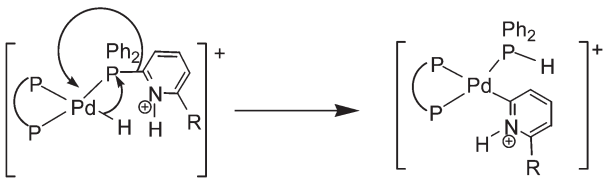

Scheme 6 Proposed mechanism for the formation of complexes **3a** and **3a-Me**.

and the structures were better described as the pyridylidene complexes.[67]

While trying to crystallize the hydride complex **Pd2a**, the light brown solution turned orange after several days at room temperature. The NMR spectra of the orange-red solid obtained after evaporation of the solvent showed very similar features to those of **Pd3a-Me**. Although we did not observe any sign of decomposition of **Pd2a** during its characterization in solution, it slowly decomposes to form the aryl complex **Pd3a**. No signs of the starting material (**Pd1a**) were detected in the solution. This observation, together with the small amounts of hydride species observed upon reaction of **Pd1a-Me** with dihydrogen, indicate that a palladium hydride is indeed an intermediate in the conversion of **Pd1a-Me** to **Pd3a-Me**.

P–C bond cleavage in palladium phosphine complexes has been widely studied because it is responsible for catalyst deactivation as well as aryl redistribution in cross-coupling reactions.[68–70] Three main mechanisms have been proposed for this reaction: oxidative addition of the phosphine-bound aryl to form a terminal phosphido group (which will usually react further to form dimeric compounds), nucleophilic attack at a coordinated phosphorus, followed by addition of the cleaved aryl group, and formation of metallophosphorane complexes.[71] In this case the oxidative addition pathway can be discarded because no phosphido bridged products were observed by ^{31}P NMR and there is no evidence of a Pd(IV) species. Metallophosphoranes have been proposed as intermediates especially when fluoride anions are involved,[72–74] but we are not aware of proven examples involving hydrides.

The hydride ligand in **Pd2a** (and the hypothetical **Pd2a-Me**) can act as an intramolecular nucleophile towards phosphorus. Because the nitrogen atom in **Pd2a** is protonated, the phosphorus–pyridinium bond is weakened, resulting in facile cleavage of this bond (Scheme 6). This mechanism would explain the observation of a P–H bond in the final product and the fact that the P–C(pyridyl) is selectively cleaved. Novak and coworkers proposed a mechanism involving reductive elimination of a phosphonium salt to give a 14-electron Pd(0) species, followed by oxidative addition of a P–C bond.[75] Although this mechanism will result in the same final product as the nucleophilic substitution mechanism, the formation of a dicationic phosphonium salt seems to be unlikely, due to the positive charge in the pyridyl moiety.

This reaction pathway is in sharp contrast to that observed for the platinum hydrides where the only decomposition observed was the loss of dihydrogen to regenerate the starting κ^2-pyridylphosphine complex. One explanation for this difference may be the stronger σ Pt–H bond compared to the Pd–H bond, which makes the nucleophilic attack at the phosphorus atom less likely in the platinum case.

Solid state structure of Pt2a-Me

Crystals suitable for X-ray diffraction were obtained by slow diffusion of diethyl ether into a dichloromethane solution of **Pt2a-Me**. Fig. 6 shows the crystal structure of $[(dppf)PtH\{2\text{-}(6\text{-}CH_3\text{-}C_5H_3NH)PPh_2\}][OTf]_2$. The most relevant bond distances and angles are presented in Table 5. The four ligands around the platinum are arranged in a plane, for which the maximum deviation from the least-squares plane defined by Pt1–H1–P1–P2–P3 is 0.089 Å. The geometry is strongly distorted from the ideal 90° angles expected for a square plane. The more

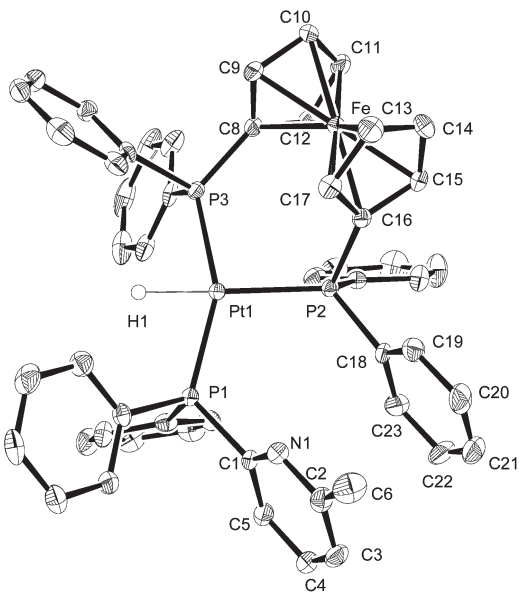

Fig. 6 Molecular structure of $[(dppf)PtH\{2\text{-}(6\text{-}CH_3\text{-}C_5H_3NH)PPh_2\}][OTf]_2\cdot CH_2Cl_2$ (**Pt2a-Me**). The displacement ellipsoids are drawn at a 50% probability level. The triflate anions, the hydrogen atoms (except for the hydride ligand) and solvent of crystallization have been omitted for clarity.

Table 5 Selected bond distances (Å) and bond angles (°) for complex **Pt2a-Me**

	Bond distances (Å)		Bond angles (°)
Pt–H1	1.64(6)	∠H1–Pt–P1	76.3(18)
Pt–P1	2.2737(11)	∠H1–Pt–P2	174.2(19)
Pt–P2	2.3410(12)	∠H1–Pt–P3	77.9(18)
Pt–P3	2.2897(11)	∠P1–Pt–P2	105.98(4)
P1–C1	1.840(4)	∠P2–Pt–P3	99.24(4)
		∠P1–Pt–P3	153.57(4)

important deviations are the H1–Pt–P1 angle (76.3(18)°) and the H1–Pt–P3 angle (77.9(18)°). The bite angle of dppf (P2–Pt–P3 is 99.24(4)°) is very similar to the 99.3(1)° observed in [(dppf)$PtCl_2$],[74] and falls within the standard range for Pt(II)–dppf complexes.[76] The preference of dppf for bite angles larger than 90° as well as the steric interaction between dppf and the 6-methyl-2-(diphenylphosphino)pyridine ligand forces P1 and P3 to bend towards the small hydride ligand, causing the rather small P1–Pt–P3 angle (153.57(4)°). The Cp rings of dppf are only slightly tilted, the angle between the two planes being 2.2°, which is relatively small for square planar complexes. The Pt–P1 and Pt–P3 bond lengths are normal for this type of Pt complex; the Pt–P3 distance of 2.2897(11) Å is in the range normally observed in (dppf)Pt(II) complexes. In contrast, the Pt–P2 bond is significantly longer (2.3410(12) Å) than other Pt–P bonds observed for phosphines *trans* to a hydride ligand, for example 2.304(3) Å in [$PtH(SiPh_3)(PEt_3)_2$][77] and 2.278(2) Å in [$PtH(CH_2CMe_3)(Cy_2PCH_2CH_2PCy_2)$].[78] The latter two complexes contain alkyl phosphines, which might explain the shorter Pt–P bond compared with the one in **Pt2a-Me**.

One of the phenyl rings of the 6-methyl-2-(diphenylphosphino)pyridine ligand (P1) is parallel to one of the phenyl rings of P2. The angle between the rings (N1, C1–C5) and (C18–C23) is only 5.5° and the distance between their centroids is 3.493 Å, which probably indicates a π-stacking interaction.

The Pt–H bond is relatively long (1.64(6) Å) compared with the one reported for [$PtH(CH_2CMe_3)(Cy_2PCH_2CH_2PCy_2)$][68] (1.56(5) Å), and to the Pt–H(terminal) distance determined by neutron diffraction in [(dppe)PtH(μ-H)$_2$Pt(dppe)]$^+$ (1.610(2)).[79]

Preliminary studies towards dihydrogen bonding and hydrogenation catalysis have been performed but only low activities were obtained (see ESI‡).

Conclusions

The coordination mode of hemilabile pyridylphosphine ligands in a series of platinum and palladium [(diphosphine)-Pt(2-(diphenylphosphino)pyridine)]$^{2+}$ complexes is determined by the steric demands of the diphosphine ligand. Thus, stable bis-chelated complexes are formed with the smaller bite angle diphosphines (dppf, DPEphos and Sixantphos) in spite of the strain imposed by the four-membered ring created by chelating 2-(diphenylphosphino)pyridine. With increasing bite angle the phenyl rings of the diphosphine "embrace" the metal center, leaving less space for other ligands, and thus destabilizing bidentate coordination of 2-(diphenylphosphino)pyridine. If the diphosphine becomes too bulky as in the case of Xantphos, P-monodentate coordination of 2-(diphenylphosphino)pyridine becomes favorable, resulting in a mixture of *cis*- and *trans*-**1d**.

A remarkable difference is observed in the reactivity of platinum and palladium complexes **1a–d** towards dihydrogen and in the stability of the product hydride complexes. Platinum complexes react smoothly with dihydrogen under mild conditions to produce stable hydride complexes **Pt2a–d**. In the case of palladium, the reaction with dihydrogen under the same conditions is fast, but the resulting hydride complexes are unstable and react further to unidentified products. The complexes bearing dppf show a remarkable difference in reactivity. While complex **Pt1a** is unable to split dihydrogen without the help of an external base, **Pd1a** is the only palladium precursor that reacts with dihydrogen in a controlled way to afford a stable hydride complex. The more bulky ligand, diphenyl-2-(6-methyl-pyridyl)phosphine, promotes the decoordination of the pyridyl moiety in both platinum and palladium complexes (**1a-Me**), thus facilitating the reaction with dihydrogen.

The platinum hydride complexes **2a–d** are stable in the solid state, but slowly lose dihydrogen in solution to regenerate the starting material. For the palladium analogs a faster reaction takes place: P–C bond cleavage of the pyridyl phosphine ligand.

Complexes **2a–d** contain a hydride as well as a proton donor in the same molecule, but no dihydrogen bonds are formed. It has been proposed that wide bite angle ligands reduce the partial negative charge on the hydride ligand.[36] In the case of **2a–d**, the decrease of the hydridic character induced by the bite angle of the diphosphines results in a too weak electrostatic interaction between the hydride and the pyridinium proton.

Experimental section

All manipulations were carried out under an argon atmosphere using standard Schlenk or glove box techniques. All solvents were dried and freshly distilled under nitrogen prior to use. Dichloromethane was distilled from CaH_2, diethyl ether, tetrahydrofuran, hexanes and pentane were distilled from sodium/benzophenone. DPEphos,[22] Sixantphos,[22] Xantphos,[22] 6-methyl-2-(diphenylphosphino)pyridine,[80] $(CH_3CN)_2PtCl_2$,[81] $(COD)PdCl_2$[82] and Na[B(3,5-(CF_3)-C_6H_3)][83] were synthesized according to literature procedures. Dppf was purchased from Aldrich Chemical Co. and used as received. 2-(Diphenylphosphino)pyridine was purchased from Aldrich Chemical Co. and re-crystallized from hot hexanes prior to use. High pressure reactions were carried out in home-made stainless steel autoclaves fitted with a glass liner, or in a Fisher-Porter bottle for reactions up to 3 bar. NMR spectra were recorded on a Bruker DPX 300, a Bruker DRX 300, a Bruker AMX 400 or a Varian

Innova 500. CD_2Cl_2 was dried over CaH_2, vacuum transferred, degassed by three freeze–thaw cycles and stored over molecular sieves. Elemental analyses were performed by the Service de Microanalyse du LCC-CNRS, Toulouse, France. X-ray diffraction studies were performed by the National NWO-CW Single Crystal Service Facility, Universiteit Utrecht, The Netherlands; or by the Service de Diffraction des Rayons X du LCC-CNRS, Toulouse, France.

dppf(2-(Diphenylphosphino)pyridine)platinum(II)bis-triflate (Pt1a)

652 mg (0.759 mmol) of (dppf)$PtCl_2$ and 511 mg (1.99 mmol) of silver triflate were dissolved in 20 mL of dry CH_2Cl_2. The color of the solution changes almost immediately from orange to deep red and a white precipitate forms. The reaction mixture was stirred for three hours with protection from light. A solution of 251 mg (0.954 mmol) of 2-(diphenylphosphino)-pyridine in 10 mL of CH_2Cl_2 was added *via* a cannula and the reaction mixture was stirred overnight. The formed AgCl was allowed to settle and the solution was filtered through celite. The clear orange solution was evaporated in vacuum and the solid obtained was re-crystallized from CH_2Cl_2/diethyl ether to yield **Pt1a** as a microcrystalline orange solid.

Yield: 950 mg (0.724 mmol), 95%.

^{1}H NMR (300 MHz, CD_2Cl_2, 295 K): 8.22 (m, 1 H, Py-H^6), 8.03–7.11 (m, 33H, Ar), 5.2, 4.86, 4.77, 3.65 (s, 8H, Cp). **^{31}P{^{1}H} NMR** (121.5 MHz, CD_2Cl_2, 295 K): −38.3 (dd, P_X, J_{PXPA} = 364 Hz, J_{PXPM} = 19 Hz, J_{PXPt} = 2058 Hz), 9.16 (t, P_M, J_{PMPA} = 12 Hz, J_{PMPt} = 3496 Hz); 24.0 (dd, P_A, J_{PAPt} = 2737 Hz). **^{13}C {^{1}H} NMR** (125.7 MHz, CD_2Cl_2, 295 K): 67.1, 71.9 (d, C_I, Cp, J_{Cp} = 77 Hz), 78.1 (d, CH, Cp, J_{Cp} = 12 Hz), 77.2 (d, CH, Cp, J_{Cp} = 9 Hz), 76.5 (d, CH, Cp, J_{Cp} = 11 Hz), 75.7 (d, CH, Cp, J_{Cp} = 8 Hz), 117.7 (d, C_I, Ph, J_{Cp} = 59 Hz), 121.5 (q, CF_3, J_{CF} = 321 Hz), 127.6 (d, C_I, Ph, J_{Cp} = 55 Hz), 129.2 (d, C_I, Ph, J_{Cp} = 70 Hz), 129.7, 129.9, 131.1, 131.3, 131.4, 133.2, 134.0, 134.1, 134.4, 134.9, 135.0 (CH, Ph), 143.5 (d, CH, Py, J_{Cp} = 5 Hz), 148.3 (d, CH, Py, J_{Cp} = 13 Hz), 170.7 (d, C_i, Py, J_{Cp} = 69 Hz).

Anal. Calcd for $C_{53}H_{42}P_3O_6NS_2F_6PtFe$: C 48.56; H 3.23. Found: C 48.13; H 3.21.

dppf(2-(Diphenylphosphino)-6-methylpyridine)platinum(II)bis-triflate (Pt1a-Me)

This compound was prepared as described for **Pt1a** using 250 mg (0.305 mmol) of (dppf)$PtCl_2$ and 196 mg (0.762 mmol) of silver triflate dissolved in 20 mL of CH_2Cl_2 and adding a solution of 93 mg (0.335 mmol) of 2-(diphenylphosphino)-6-methylpyridine in 5 mL of CH_2Cl_2. Yield: 354 mg (0.275 mmol), 90%.

^{1}H NMR (300 MHz, CD_2Cl_2, 233 K): 8.10–6.67 (m, Ar, both products); 5.03, 4.90, 4.75, 4.71 (s, 2H each, Cp prod. 2); 4.37, 4.29, 3.31 (s, 8H total, Cp product 1); 2.48 (s, 3H, CH_3 prod. 2); 1.72 (s, 3H, CH_3, prod. 1). **^{31}P{^{1}H} NMR** (121.5 MHz, CD_2Cl_2, 233 K): Product 1, AMX spin system: −40.0 (dd, P_X, J_{PXPA} = 354 Hz, J_{PXPM} = 20.7 Hz, J_{PXPt} = 2075 Hz); 5.04 (dd, P_M, J_{PMPA} = 12.2 Hz, J_{PMPt} = 3533 Hz); 20.9 (dd, P_A, J_{PAPt} = 2728 Hz). Product 2, ABX spin system: 15.84 (dd, P_x, J_{PxPA} = 14.6 Hz, J_{PxPB} = 19.4 Hz, J_{PXPt} = 3764 Hz); 16.38 (AB, P_A, J_{PAPB} = 425 Hz, J_{PAPt} = 3461 Hz); 23.23 (AB, P_B, J_{PBPt} = 2538 Hz). IR (KBr pellet): $\nu(SO_3)$ 1260 and 1005 cm^{-1}.

Anal. Calcd for $C_{54}H_{44}P_3O_6NS_2F_6PtFe$: C 48.97; H 3.35. Found: C 48.85; H 3.37.

DPEphos(2-(diphenylphosphino)pyridine)platinum(II)bis-triflate (Pt1b)

This compound was prepared as described for **1a** using 125 mg (0.157 mmol) of (DPEphos)$PtCl_2$ and 100 mg (0.392 mmol) of silver triflate in 10 mL of CH_2Cl_2. The reaction mixture changed from colorless to bright yellow. After 3 hours of stirring 45.4 mg (0.172 mmol) of 2-(diphenylphosphino)pyridine in 5 mL of CH_2Cl_2 were added *via* a cannula, and the reaction mixture turned pale yellow. The light gray solid obtained was recrystallized from CH_2Cl_2/diethyl ether to yield **1b** as a white powder.

Yield: 180 mg (90%). Crystals suitable for X-ray analysis were obtained by layering a concentrated CH_2Cl_2 solution of the pure product with 20 mL of hexane.

^{1}H NMR (300 MHz, CD_2Cl_2, 295 K): 8.23 (m, 1 H, Py-H^6), 7.98–6.80 (m, 39H, Ar), 6.66 (m, ^{1}H, Py-H^5), 6.38 (m, ^{1}H, Py-H^3). **^{31}P{^{1}H} NMR** (121.5 MHz, CD_2Cl_2, 295 K): −39.2 (dd, P_X, J_{PXPA} = 372 Hz, J_{PXPM} = 15.8 Hz, J_{PXPt} = 2143 Hz); −7.5 (t, P_M, $J_{PMPA/X}$ = 16.3 Hz, J_{PMPt} = 3536 Hz); 15.8 (dd, P_A, J_{PAPt} = 2829 Hz). **^{13}C {^{1}H}** NMR (75.5 MHz, CD_2Cl_2, 295 K): 118.0, 118.4, 118.7 (C_I), 119.0 (d, CH, J_{Cp} = 7.5 Hz), 121.5 (q, CF_3, J_{CF} = 321.5 Hz), 123.4, 125.9 (C_I), 125.9, 126.1 (CH), 127.5 (d, CH, J_{Cp} = 7.5 Hz), 126.5 (d, C_I, J_{Cp} = 38.1 Hz), 129.9, 130.8, 131.1, 133.2, 133.5, 133.7, 133.9, 134.4, 134.8, 135.6, 136.1, 137.7, 143.5 (d, CH, Py, J_{Cp} = 5.0 Hz), 148.5 (d, CH, Py, J_{Cp} = 8.0 Hz), 158.9, 159.1 (d, C–O, J_{CP} = 7 Hz), 170.4 (d, C_i, Py, J_{Cp} = 67.9 Hz).

Anal. Calcd for $C_{55}H_{42}P_3O_7NS_2F_6Pt$: C 50.90; H 3.20. Found: C 50.37; H 3.01.

Sixantphos(2-(diphenylphosphino)pyridine)platinum(II)bis-triflate (Pt1c)

This compound was prepared as described for **Pt1a** using 502 mg (0.583 mmol) of (Sixantphos)$PtCl_2$ and 374.8 mg (1.46 mmol) of silver triflate in 25 mL of CH_2Cl_2, and adding 169 mg (0.642 mmol) of 2-(diphenylphosphino)pyridine in 10 mL of CH_2Cl_2. A yellow solid was obtained and recrystallized from CH_2Cl_2/pentane to yield **1c** as a white microcrystalline solid. Yield: 696 mg (0.515 mmol), 88%. Crystals suitable for X-ray analysis were obtained by slow diffusion of pentane into a concentrated CH_2Cl_2 solution of the pure product, at room temperature.

^{1}H NMR (300 MHz, CD_2Cl_2, 295 K): 8.20 (m, 1 H, Py-H^6), 8.05–6.97 (m, 38 H, Ar), 6.82 (m, ^{1}H, Py-H^3), 0.77 (s, 6H, CH_3). **^{31}P{^{1}H} NMR** (CD_2Cl_2 at 295 K): −40.1 (dd, P_X, J_{PXPA} = 360 Hz, J_{PXPM} = 15.2 Hz, J_{PXPt} = 2142 Hz); −6.6 (t, P_M, $J_{PMPA/X}$ = 19.3 Hz, J_{PMPt} = 3563 Hz); 12.8 (dd, P_A, J_{PAPt} = 2772 Hz). **^{13}C {^{1}H} NMR** (125.7 MHz, CD_2Cl_2, 295 K): −2.4 (s, Si–CH_3), 114.3 (d, C_I, J_{Cp} = 66.5 Hz) 115.7 (d, C_I, J_{Cp} = 69.3 Hz), 121.5 (q, CF_3, J_{CF} = 321.5 Hz), 126.0 (d, C_I, C–O, J_{Cp} = 15.1 Hz), 126.2 (d, CH, J_{Cp} =

7.8 Hz), 126.5 (d, C_I, J_{Cp} = 38.1 Hz), 127.3, 129.8, 129.9, 130.1, 131.0, 131.1, 133.0, 133.3, 133.9, 134.2, 134.6, 135.7, 139.5, 139.8, 143.2 (d, CH, Py, J_{Cp} = 5.0 Hz), 148.9 (d, CH, Py, J_{Cp} = 13.0 Hz), 170.7 (d, C_i, Py, J_{Cp} = 56.4 Hz).

Anal. Calcd for $C_{57}H_{46}P_3O_7NS_2F_6SiPt{\cdot}CH_2Cl_2$: C 49.0; H 3.21. Found: C 49.71; H 3.40.

Xantphos(2-(diphenylphosphino)pyridine)platinum(II)bis-triflate (Pt1d)

This compound was prepared as described for **Pt1a** using 250 mg (0.296 mmol) of (Xantphos)$PtCl_2$ and 190.2 mg (0.740 mmol) of silver triflate in 15 mL of CH_2Cl_2, and adding 86 mg (0.330 mmol) of 2-(diphenylphosphino)pyridine in 5 mL of CH_2Cl_2. A yellow solid is obtained and recrystallized from CH_2Cl_2/ether to yield **1d** as a light yellow powder. Yield: 335 mg (0.251 mmol) 85%. Crystals suitable for X-ray analysis were obtained by layering a concentrated CH_2Cl_2 solution of the pure product with 10 mL of hexane.

^{1}H NMR (300 MHz, CD_2Cl_2, 295 K): 8.44–6.12 (m, Ar, 40H); 1.95 (s, CH_3, *cis* prod.); 1.72 (s, CH_3, **1d**-*trans*); 1.62 (s, CH_3, **1d**-*cis*), 6H total for the three signals. **^{31}P{^{1}H} NMR** (121.5 MHz, CD_2Cl_2, 295 K): **1d**-*cis*: −41.3 (dd, P_X, J_{PXPA} = 358 Hz, J_{PXPM} = 12.2 Hz, J_{PXPt} = 2118 Hz); −6.5 (dd, P_M, J_{PMPA} = 24.3 Hz, J_{PMPt} = 3654 Hz); 12.0 (dd, P_A, J_{PAPt} = 2800 Hz). **1d**-*trans*: 16.3 (t, P_X, J_{PAPx} = 12.1 Hz, J_{PXPt} = 4447 Hz), 39.2 (d, P_A, 2P, J_{PAPt} = 2503 Hz).

Anal. Calcd for $C_{58}H_{46}P_3O_7NS_2F_6Pt$: C 52.18; H 3.47; N 1.05. Found: C 52.05; H 3.35.

dppf(2-(Diphenylphosphino)pyridine)palladium(II)bis-triflate (Pd1a)

150 mg (0.205 mmol) of (dppf)$PdCl_2$ and 132 mg (0.512 mmol) of silver triflate were dissolved in 10 mL of CH_2Cl_2 in a Schlenk tube protected from light. The color of the solution changed immediately from orange to deep green and a white precipitate was formed. The reaction mixture was stirred for 1 hour. The AgCl formed is allowed to settle and the solution was filtered into a Schlenk flask containing a solution of 65 mg (0.246 mmol) of diphenylphosphino-2-pyridine in 5 mL of CH_2Cl_2. The color of the solution changed from green to purple. The reaction mixture was stirred for two hours and the solution was filtered over celite. The deep purple solution was evaporated in a vacuum and the solid obtained was washed with diethyl ether (2 × 5 mL) to yield **Pd1a** as a purple solid. The crude product was re-crystallised from CH_2Cl_2/Et_2O to obtain pure **Pd1a**.

Yield = 200 mg (0.164 mmol), 80%.

^{1}H NMR (300 MHz, CD_2Cl_2, 295 K): 8.08 (m, 1 H, Py-H^6), 7.97–7.07 (m, 33H, Ar), 5.28 (s, 2H, αH Cp), 4.84 (s, 2H, βH Cp), 4.47 (s, 2H, βH Cp), 3.65 (s, 2H, αH Cp). **^{31}P{^{1}H} NMR** (121.5 MHz, CD_2Cl_2, 295 K): −42.3 (dd, P_X, J_{PXPA} = 408 Hz, J_{PXPM} = 14 Hz), 30.7 (dd, P_A, J_{PAPM} = 8.5 Hz), 41.7 (t, P_M). **^{13}C {^{1}H} NMR** (125.7 MHz, CD_2Cl_2, 295 K): 148.4, 142.3 (CH, Py); 134.7, 134.6, 134.5, 134.1, 133.8, 133.6, 133.5, 133.3, 130.9, 130.8, 130.7, 130.6, 129.6, 129.5 (CH, Ar); 130.3, 129.8, 127.8, 127.5 (C_I, Ph); 121.2 (q, CF_3, J_{CF} = 321.1 Hz); 119.7, 119.3 (C_I, Ph); 79.5 (d, CH, Cp, J_{CP} = 12.7 Hz); 77.2 (d, CH, Cp, J_{CP} = 9.4 Hz); 76.7 (d, CH, Cp, J_{CP} = 9.3 Hz); 76.1 (d, CH, Cp, J_{CP} = 10.6 Hz); 75.2 (d, CH, Cp, J_{CP} = 7.6 Hz); 75.1 (d, C_I, Cp, J_{CP} = 66.3 Hz); 66.0 (d, C_I, Cp, J_{CP} = 58.5 Hz).

Anal. Calcd for $C_{53}H_{42}P_3O_6NS_2F_6PdFe$: C 52.09; H 3.46. Found: C 52.12; H 3.50.

During the crystallization of this compound, orange plates were obtained by slow diffusion of pentane into a solution of **Pd1a** in THF. X-ray analysis of the crystals revealed that they corresponded to [Pd(μ-2-(diphenylphosphino)pyridine)OTf]$_2$.

dppf(2-(Diphenylphosphino)-6-methylpyridine)palladium(II)-bis-triflate (Pd1a-Me)

This compound was prepared using the same procedure as described for **1a** using 200 mg (0.273 mmol) of dppf$PdCl_2$ and 176 mg (0.683 mmol) of AgOTf in 10 mL of CH_2Cl_2, and 83.3 mg (0.301 mmol) of 2-(diphenylphosphino)-6-methylpyridine in 5 mL of CH_2Cl_2. After working-up as for **Pd1a**, a dark brown microcrystalline solid was obtained. Repeated crystallization from CH_2Cl_2/pentane was necessary to obtain a pure product.

Yield = 260 mg (0.210 mmol), 77%.

^{1}H NMR (300 MHz, CD_2Cl_2, 233 K): 7.93–7.00 (br. m, 33H, Ar), 4.77 (s, 2H, Cp), 4.69 (s, 2H, H Cp), 4.33 (br. s, 4H, Cp), 1.61 (br. s, 3H, CH_3). **^{31}P{^{1}H} NMR** (121.5 MHz, CD_2Cl_2, 233 K): −43.6 (d, P_X, J_{PXPA} = 400 Hz), 25.0 (d, P_A), 40.3 (P_M). **^{13}C {^{1}H} NMR** (125.7 MHz, CD_2Cl_2, 193 K): 166.0 (d, C_i, Py, J_{CP} = 66.4 Hz); 162.1 (d, C_i, Py, J_{CP} = 13.8 Hz); 141.9 (CH, Py); 134.4, 133.8, 133.5, 132.7, 131.0, 130.9, 131.3, 130.2, 129.4, 129.2, 128.7 (CH, Ar); 128.9, 119.1, 118.8 (C_I, Ar); 120.7 (q, CF_3, J_{CF} = 320.7 Hz); 119.7, 119.3 (C_I, Ph); 79.1 (m, CH, Cp); 71.6 (d, C_I, Cp, J_{CP} = 74.4 Hz); 69.3 (d, C_I, Cp, J_{CP} = 59.8 Hz); 24.9 (CH_3).

This product contained small amounts of [(κ^3-dppf)Pd(κ^1-(2-(diphenylphosphino)-6-methylpyridine))][OTf]$_2$.

^{31}P{^{1}H} NMR (121.5 MHz, CD_2Cl_2, 233 K): 42.3 (t, PPh_2Py, J_{pp} = 13.2 Hz); −14.9 (d, κ^3-dppf).

Anal. Calcd for $C_{54}H_{44}P_3O_6NS_2F_6PdFe$: C 52.47; H 3.59. Found: C 52.67; H 3.62.

DPEphos(2-(diphenylphosphino)pyridine)palladium(II)bis-triflate (Pd1b)

126 mg (0.176 mmol) of (DPEphos)$PdCl_2$ were suspended in 15 mL of CH_2Cl_2 and 113 mg (0.440 mmol) of silver triflate in 5 mL of CH_2Cl_2 were added. The dark yellow suspension was stirred overnight after which a bright orange solution had formed. The AgCl formed was allowed to precipitate and the solution was filtered into a Schlenk flask containing 55.6 mg (0.211 mmol) of 2-(diphenylphosphino)pyridine in 5 mL of CH_2Cl_2. The reaction mixture was stirred for 16 h. The same work-up procedure as for **Pd1a** was used to obtain **Pd1b** as a fluffy bright yellow solid. Yield = 181 mg (0.150 mmol), 85%.

^{1}H NMR (300 MHz, CD_2Cl_2, 295 K): 9.2 (m, 1H, Py-H^6), 8.05–6.72 (m, 40H, Ar), 6.56 (m, ^{1}H, Py-H^3). **^{31}P{^{1}H} NMR** (121.5 MHz, CD_2Cl_2, 295 K): −46.0 (dd, P_X, J_{PXPA} = 412 Hz), 20.05 (t, P_M), 20.49 (dd, P_A, J_{PAPM} = 3.7 Hz). **^{13}C {^{1}H} NMR** (125.7 MHz, CD_2Cl_2, 295 K): 169.1 (d, C_i, Py, J_{CP} = 86.1 Hz);

159.2, 158.3 (d, C–O); 148.8 (d, CH, Py, J_{CP} = 12.2 Hz); 142.4 (CH, Py); 139.9, 136.6, 135.7, 135.1 (CH, Ar); 134.8 (d, CH, J_{CP} = 11.8 Hz); 134.5 (d, CH, J_{CP} = 10.9 Hz); 134.2, 134.0 (d, CH, J_{CP} = 2.9 Hz); 133.7 (d, CH, J_{CP} = 11.4 Hz); 133.3, 132.9, 132.3, 131.5 (d, CH, J_{CP} = 4.6 Hz); 130.8 (d, CH, J_{CP} = 11.81 Hz); 130.3 (d, CH, J_{CP} = 11.4 Hz); 130.1, 129.9, 129.6 (d, CH, J_{CP} = 12.2 Hz); 128.9, 127.1 (d, CH, J_{CP} = 8.9 Hz); 126.0 (d, CH, J_{CP} = 8.4 Hz); 125.0 (d, CH, J_{CP} = 5.5 Hz); 127.4, 126.9, 125.9 (C_I); 125.6 (d, C_I, J_{Cp} = 12.0 Hz); 121.5 (q, CF_3, J_{CF} = 321.5 Hz); 120.7 (d, C_I, J_{Cp} = 12.5 Hz); 120.3, 120.1, 119.7, 119.2, 118.77 (C_I).

Anal. Calcd for $C_{55}H_{42}P_3O_7NS_2F_6Pd$: C 54.76; H 3.51. Found: C 55.01; H 3.62.

Xantphos(2-(diphenylphosphino)pyridine)palladium(II)bis-triflate (Pd1d)

This compound was prepared using the same procedure as described for **Pd1b** using 231 mg (0.306 mmol) of XantphosPdCl_2 and 196 mg (0.764 mmol) of AgOTf and 96.6 mg (0.367 mmol) of 2-(diphenylphosphino)pyridine in 5 mL of CH_2Cl_2. The same work-up procedure as for **1a** was used to obtain an orange-yellow solid.

Yield = 362 mg (0.362 mmol), 90%.

^{1}H NMR (CD_2Cl_2 at 233 K, a mixture of *cis* and *trans* complexes: 8.42–6.09 (m, 66H, Ar), 1.91 (s, 1.2H, CH_3 *cis*), 1.72 (s, 6H, CH_3 *trans*), 1.55 (s, 1.2H, CH_3 *cis*). **^{31}P{^{1}H} NMR** (CD_2Cl_2 at 233 K), *cis* product: −45.1 (d, P_X, J_{PXPA} = 388 Hz), 12.9 (dd, P_A, J_{PAPM} = 4.9 Hz), 18.8 (t, P_M). *trans* product: 35.1 (br, t, P_X), 36.2 (d, P_A, J_{PAPX} = 23.1 Hz).

Anal. Calcd for $C_{56}H_{46}P_3O_7NS_2F_6Pd$: C 55.02; H 3.79. Found: C 55.10; H 3.92.

dppf(2-(Diphenylphosphino)pyridine)hydridoplatinum(II)bis-triflate (Pt2a)

43 μL of diethylamine were added to a solution of 540 mg (0.412 mmol) of **Pt1a** in 20 mL CH_2Cl_2. This solution was introduced into a stainless steal autoclave under argon, and purged 3 times with H_2, after which the autoclave was pressurized to 4 bar of H_2 and heated to 40 °C overnight. After reducing the pressure to 1 bar and cooling to room temperature, the reaction mixture was transferred to a Schlenk flask under 1 bar of H_2. The yellow brown solution was evaporated under vacuum to obtain an amber sticky solid, which after thorough washing with diethyl ether (5 × 10 mL) and drying under vacuum afforded a golden powder. The ammonium salt was removed by crystallization from CH_2Cl_2/Et_2O.

100 mg (0.076 mmol) of this complex was dissolved in 10 mL of CH_2Cl_2 and the solution was frozen in an acetone/liquid nitrogen bath. 10.1 μL (17.16 mg, 0.114 mmol) of HOTf were added using a microsyringe. The Schlenk flask was shaken to dissolve the acid and the reaction mixture was slowly warmed to room temperature. After 1 h at room temperature, the solvent was evaporated in a vacuum. The oily orange product was washed several times with diethyl ether to obtain a dark orange solid. Yield: 80 mg (0.061 mmol), 72%.

^{1}H NMR (300 MHz, CD_2Cl_2, 295 K): 15.1 (br, NH), 8.54 (br, 1H, Py-H^6), 8.35 (br, ^{1}H), 7.84–7.07 (m, 32H, Ar), 4.87 (s, 2H, Cp); 4.61 (s, 2H, Cp); 4.30 (s, 2H, Cp); 3.62 (s, 2H, Cp); −5.72 (s, 1H, hydride, J_{HPA} = 11.7, J_{HPB} = 18.45 Hz, J_{HPX} = 154 Hz J_{HPt} = 762 Hz). **^{31}P{^{1}H} NMR** (121.5 MHz, CD_2Cl_2, 295 K): 22.9 (P_X, J_{PXPA} = 10.81 Hz, J_{PXPB} = −8.8 Hz, J_{PxPt} = 2310 Hz); 21.8 (P_B, J_{PAPB} = 364 Hz, J_{PBPt} = 2755 Hz); 28.7 (P_A, J_{PAPt} = 3033 Hz). IR ν(Pt–H) = 2078 cm^{-1}.

dppf(2-(Diphenylphosphino)-6-methylpyridine)-hydridoplatinum(II)bis-triflate (Pt2a-Me)

100 mg (0.075 mmol) of **Pt1a-Me** were dissolved in 10 mL of CH_2Cl_2 and introduced into a stainless steel autoclave under Ar and purged 3 times with H_2. The autoclave was pressurized to 4 bar of H_2 and heated to 40 °C overnight. After cooling to room temperature and reducing the pressure to 1 bar, the reaction mixture was transferred to a Schlenk flask under 1 bar of H_2. The orange solution was evaporated under vacuum and the remaining solid was washed with 10 mL of pentane and re-crystallized from CH_2Cl_2/Et_2O to afford **Pt2a-Me** as a dark orange solid. Yield: 93 mg (0.070 mmol), 93%.

^{1}H NMR (300 MHz, CD_2Cl_2, 295 K): hydride region, **2a-Me** *cis* −5.61 (ddd, J_{HPA} = 10.5 Hz, J_{HPB} = 22.5 Hz, J_{HPX} = 150.0 Hz, J_{HPt} = 750 Hz). **2a-Me** *trans* −5.11 (dt, J_{HPA} = 13.5 Hz, J_{HPX} = 162.0 Hz, J_{HPt} = 797 Hz). **^{31}P{^{1}H} NMR** (121.5 MHz, CD_2Cl_2, 295 K): **2a-Me** *cis*, 20.7 (P_B, J_{PAPB} = 372 Hz, J_{PBPX} = −21.9 Hz, J_{PBPt} = 3079 Hz), 23.6 (P_X, J_{PXPA} = 18.2 Hz, J_{PxPt} = 2395 Hz), 29.9 (P_A, J_{PAPt} = 2750 Hz). **2a-Me** *trans*, 22.9 (P_X, J_{PXPA} = 19.4 Hz, J_{PxPt} = 2255 Hz), 25.3 (P_A, J_{PAPt} = 2863 Hz).

DPEphos(2-(diphenylphosphino)pyridine)hydridoplatinum(II)-bis-triflate (Pt2b)

This compound was prepared as described for **Pt2a-Me** using 200 mg (0.155 mmol) of **Pt1b** dissolved in 20 mL of CH_2Cl_2. The crude off-white solid was washed with 10 mL of pentane and re-crystallized from CH_2Cl_2/Et_2O to afford pure **Pt2b** as a white solid. Yield: 170 mg (0.131 mmol), 85%.

^{1}H NMR (300 MHz, CD_2Cl_2, 295 K): 8.50 (d, 1H, Py-H^6), 7.77–6.87 (m, 38H, Ar), 6.78 (t, 1H, Py, J = 7.3 Hz), 6.61 (t, 1H, Py, J = 9.5 Hz), 6.07 (m, 1H, Py), −6.81 (s, 1H, hydride, J_{HPA} = 13.0 Hz, J_{HPB} = 16.5 Hz, J_{HPX} = 163.1 Hz, J_{HPt} = 739 Hz). **^{31}P{^{1}H} NMR** (121.5 MHz, CD_2Cl_2, 295 K): 16.4 (P_B, J_{PAPB} = 361 Hz, J_{PBPX} = −10.5 Hz, J_{PBPt} = 2944 Hz); 16.5 (P_X, J_{PXPA} = 31.7 Hz, J_{PxPt} = 2217 Hz); 23.4 (P_A, J_{PAPt} = 2905 Hz).

Anal. Calcd for $C_{55}H_{44}P_3O_7NS_2F_6Pt$: C 50.93; H 3.42. Found: C 51.05; H 3.45.

Sixantphos(2-(diphenylphosphino)pyridine)hydridoplatinum(II)-bis-triflate (Pt2c)

This compound was prepared as described for **Pt2a-Me** using 200 mg (0.148 mmol) of **Pt1c**. The crude off-white product was re-crystallized from CH_2Cl_2/pentane to afford pure **Pt2c** as a white solid. Yield: 180 mg (0.133 mmol), 90%.

^{1}H NMR (300 MHz, CD_2Cl_2, 295 K): 15.1 (br, NH), 9.12 (m, 1 H, Py-H^6), 8.50–6.75 (m, 39 H, Ar), 0.75 (s, 6H, CH_3), −7.53 (s, 1H, hydride, J_{HPA} = 13.7 Hz, J_{HPB} = 14.7 Hz, J_{HPX} = 158 Hz,

J_{HPt} = 732 Hz). **$^{31}P\{^1H\}$ NMR** (121.5 MHz, CD_2Cl_2, 295 K): 15.9 (P_X, J_{PXPA} = −12.7 Hz, J_{PXPB} = 24.3 Hz, J_{PxPt} = 2286 Hz), 20.1 (P_B, J_{PAPB} = 370 Hz, J_{PBPt} = 2030 Hz), 23.8 (P_A, J_{PAPt} = 2922 Hz). **^{195}Pt NMR** (HMQC, 85.6 MHz, CD_2Cl_2, 273 K): −5090.

Anal. Calcd for $C_{57}H_{48}P_3O_7NS_2F_6SiPt{\cdot}CH_2Cl_2$: C 48.94; H 3.34. Found: C 49.14; H 3.13.

Xantphos(2-(diphenylphosphino)pyridine)hydridoplatinum(II)-bis-triflate (Pt2d)

This compound was prepared as described for **Pt2a-Me** using 250 mg (0.187 mmol) of **Pt1d**. The crude pale yellow product was re-crystallized from CH_2Cl_2/pentane to afford pure **Pt2d** as a white solid. Yield: 230 mg (0.172 mmol), 92%.

^{1}H NMR (300 MHz, CD_2Cl_2, 295 K): 15.4 (br, NH), 9.17 (m, 1 H, Py-H^6), 8.50–6.90 (m, 39 H, Ar), 1.83 (s, 6H, CH_3), −8.41 (s, 1H, hydride, J_{HPA} = J_{HPB} = 14.4 Hz, J_{HPX} = 159 Hz, J_{HPt} = 714 Hz). **$^{31}P\{^1H\}$ NMR** (121.5 MHz, CD_2Cl_2, 295 K): 15.8 (P_X, J_{PXPA} = 16.3 Hz, J_{PXPB} = −19.6 Hz, J_{PxPt} = 2298 Hz), 17.7 (P_B, J_{PAPB} = 375 Hz, J_{PBPt} = 2937 Hz); 23.0 (P_A, J_{PBPt} = 3045 Hz). **^{195}Pt NMR** (HMQC, 64.19 MHz, CD_2Cl_2, 273 K): −5090. IR ν(Pt–H) = 2099 cm^{-1}.

Anal. Calcd for $C_{58}H_{48}P_3O_7NS_2F_6Pt$: C 52.1; H 3.6. Found: C 51.72; H 3.50.

High pressure NMR experiments

In a typical experiment the high pressure sapphire NMR tube was charged with the corresponding starting material (**1a–d**) and 2 mL of CD_2Cl_2 were added inside a glove box. The closed tube was then taken out of the box, cooled in an ethanol/N_2 bath when necessary, and pressurized with H_2. The tube was then transferred to the pre-cooled NMR probe at the desired temperature. The reactions were followed in time by ^{1}H and ^{31}P NMR spectroscopy.

dppf(2-(Diphenylphosphino)pyridine)hydridopalladium(II)bis-triflate (Pd2a)

68 mg (0.056 mmol) of **Pd1a** were dissolved in 20 mL of CH_2Cl_2 and the purple solution was transferred to an autoclave under Ar. The autoclave was pressurized to 10 bar of H_2 and the solution was allowed to react during 65 hours. The reaction mixture was transferred to a Schlenk tube using H_2 pressure and the solvent was evaporated with a stream of H_2. The resulting light brown solid was washed with pentane (3 × 5 mL.) and finally dried under vacuum. Yield = 50 mg (0.041 mmol), 73.4%.

^{1}H NMR (300 MHz, CD_2Cl_2, 295 K): 15.1 (br., 1 H, NH), 8.5–7.1 (m, 34H, Ar), 4.96 (s, 2H, Cp), 4.64 (s, 2H, Cp), 4.33 (s, 2H, Cp), 3.69 (s, 2H, Cp), −6.7 (dd, J_{HPX} = 171 Hz, $J_{HPA/PB}$ = 16, hydride). **$^{31}P\{^1H\}$ NMR** (121.5 MHz, CD_2Cl_2, 295 K): 22.63 (t, P_X, $J_{PXPA/B}$ = 26.9 Hz), 32.22 (dd, $P_{A/B}$).

Anal. Calcd for $C_{54}H_{46}P_3O_6NS_2F_6PdFe$: C 52.00; H 3.62. Found: C 51.86; H 3.58.

dppf(2-Diphenyphosphine)(pyridinium)palladium(II)bis-triflate (Pd3a)

This compound was obtained during the crystallization of **Pd2a** from CH_2Cl_2/Et_2O at room temperature.

^{1}H NMR (300 MHz, CD_2Cl_2, 295 K): 13.5 (br., 1 H, NH), 7.9–7.07 (m, 34H, Ar), 6.0 ppm (ddd, P–H, $^1J_{HP}$ = 370 Hz, $^3J_{HP}$ = 16.8, 10.2 Hz), 5.16 (s, 1H, Cp), 4.76 (s, 1H, Cp), 4.65 (s, 2H, Cp), 3.39 (s, 1H, Cp), 4.33 (s, 1H, Cp), 4.15 (s, 1H, Cp), 3.82 (s, 1H, Cp). **$^{31}P\{^1H\}$ NMR** (121.5 MHz, CD_2Cl_2, 295 K): −1.6 (dd, P_X, J_{PXPA} = 354 Hz, J_{PXPM} = 34.0 Hz), 17.86 (dd, P_M, J_{PMPX} = 14.6 Hz), 26.71 (dd, P_A).

dppf(2-Diphenyphosphine)(6-methyl-pyridinium)palladium(II)-bis-triflate (Pd3a-Me)

A Fisher–Porter bottle equipped with a magnetic stirring bar was charged with 95 mg (0.077 mmol) of **Pd1a-Me** and 10 mL of CH_2Cl_2 were added. The dark-brown solution was cooled in an ice bath and the bottle was pressurized with 3 bar of H_2. The solution became light brown almost immediately and after 15 min, it turned bright red. The solution was kept under pressure for an additional 15 min and then transferred into a Schlenk tube. The solvent was evaporated in a vacuum, the remaining solid was washed with pentane (3 × 5 mL) and dried under vacuum. Yield = 71.4 mg (0.058 mmol), 75%.

^{1}H NMR (300 MHz, CD_2Cl_2, 193 K): 12.05 (br., 1H, NH), 9.31–7.04 (m, 34H, Ar), 6.1 ppm (ddd, P–H, $^1J_{HP}$ = 375 Hz, $^3J_{HP}$ = 16.8, 10.2 Hz), 5.21 (s, 1H, Cp), 4.69 (s, 1H, Cp), 4.48 (s, 4H, Cp), 4.41 (s, 1H, Cp), 4.35 (s, 1H, Cp), 3.79 (s, 1H, Cp), 1.53 (s, 3H, CH_3). **$^{31}P\{^1H\}$ NMR** (121.5 MHz, CD_2Cl_2, 193 K): −2.2 (dd, P_X, J_{PXPA} = 350 Hz, J_{PXPM} = 36.5 Hz), 17.7 (dd, P_M, J_{PMPX} = 12.1 Hz), 27.2 (dd, P_A). **^{13}C $\{^1H\}$ NMR** (100.6 MHz, CD_2Cl_2, 233 K): 179.5 (dt, C2 Py, $J_{CPtrans}$ = 125.5 Hz, J_{CPcis} = 12.6 Hz); 157.1 (d, C_6 Py, J_{CP} = 4.7 Hz); 141.2 (CH, Py); 136.3 (d, CH, J_{CP} = 11.5 Hz); 134.8, 135.5, 134.3, 132.9, 132.6 (CH, Ar); 132.9 (d, CH, J_{CP} = 52.4 Hz); 131.9, 131.7, 131.5, 131.3 (d, CH, J_{CP} = 9.8 Hz); 130.7 (d, CH, J_{CP} = 9.7 Hz); 130.5, 130.3 (d, CH, J_{CP} = 11.1 Hz); 129.9 (d, CH, J_{CP} = 11.1 Hz); 129.6 (d, CH, J_{CP} = 9.2 Hz); 128.8, 128.6 (d, CH, J_{CP} = 11.5 Hz); 128.2, 125.7, 125.2, 124.6 (C_{quat}); 122.4 (CH); 121.0 (q, CF_3, J_{CF} = 320.1 Hz); 120.8 (C_{quat}, J_{CP} = 51.9 Hz); 78.6 (d, CH, Cp, J_{CP} = 22.2 Hz); 77.4 (d, CH, Cp, J_{CP} = 11.2 Hz); 76.9 (d, CH, Cp, J_{CP} = 7.6 Hz); 76.3 (d, CH, Cp, J_{CP} = 4.2 Hz); 75.3 (d, CH, Cp); 74.3 (d, CH, Cp, J_{CP} = 13.9 Hz); 74.0 (d, CH, Cp, J_{CP} = 5.9 Hz); 72.6 (d, CH, Cp, J_{CP} = 5.4 Hz); 70.6 (d, C_I, Cp, J_{CP} = 59.5 Hz); 70.2 (d, C_I, Cp, J_{CP} = 51.8 Hz); 20.1 (CH_3).

Anal. Calcd for $C_{54}H_{44}P_3O_6NS_2F_6PdFe$: C 52.38; H 3.74. Found: C 52.35; H 3.59.

X-ray structures of Pt1b, Pt1c, *trans*1d and Pt2a-Me

Pertinent data on the crystal structures have been deposited with the CCDC (904331–904334). Pt1b crystallizes in space group $P\bar{1}$ with three molecules of dichloromethane. X-ray data were collected on an Enraf-Nonius CAD4T diffractometer on a rotating anode (MoKα) at 150 K. One of the triflate anions was refined with a disorder model. R_1 = 0.0669, wR_2 = 0.178, S =

1.029. **Pt1c** crystallizes in space group *C*2/*c* with one dichloromethane, distributed over two locations of which one disordered. X-ray data were collected on a Stoe IPDS (MoKα) system at 180 K. The H-atoms of CH_2Cl_2 were not included in the model and refinement. R_1 = 0.0395, wR_2 = 0.1015, S = 1.045. ***trans*1d** crystallizes in space group *C*2/*c* with half a H_2O molecule. X-ray data were collected on a Nonius KappaCCD on a rotating anode (MoKα) at 150 K. R_1 = 0.0224, wR_2 = 0.0562, S = 1.007. **Pt2a-Me** crystallizes in space group $P2_1/c$ with one CH_2Cl_2 molecule of crystallization. X-ray data were collected on a Nonius KappaCCD on a rotating anode (MoKα) at 150 K.

Acknowledgements

The work described here was financially supported by the Council for Chemical Sciences of the Netherlands Organization for Scientific Research (CW-NWO).

References

1 (*a*) G. J. Kubas, *Metal Dihydrogen and Sigma-Bond Complexes*, Kluwer Academic/Plenum Publishers, New York, 2001; (*b*) X. Fang, B. I. Scott, K. D. John and G. J. Kubas, *Organometallics*, 2000, **19**, 4141; (*c*) X. Fang, B. I. Scott, J. G. Watkin and G. J. Kubas, *Organometallics*, 2000, **19**, 4193; (*d*) G. J. Kubas, *Chem. Rev.*, 2007, **107**, 4152.
2 J. Y. Corey and J. Braddock-Wilking, *Chem. Rev.*, 1999, **99**, 175.
3 (*a*) F. Delpech, S. Sabo-Etienne, J.-C. Daran, B. Chaudret, K. Hussein, C. J. Marsden and J.-C. Barthelat, *J. Am. Chem. Soc.*, 1999, **121**, 6668; (*b*) R. N. Perutz and S. Sabo-Etienne, *Angew. Chem., Int. Ed.*, 2007, **46**, 2578.
4 M. W. W. Adams and E. I. Stiefel, *Science*, 1998, **282**, 1842.
5 (*a*) R. Cammack, *Nature*, 1999, **397**, 214; (*b*) A. L. De Lacey, V. M. Fernandez, M. Rousset and R. Cammack, *Chem. Rev.*, 2007, **107**, 4304.
6 J. Y. Yang, R. Morris Bullock, M. Rakowski DuBois and D. L. DuBois, *MRS Bull.*, 2011, **36**, 39.
7 (*a*) B. K. Burgess and D. J. Lowe, *Chem. Rev.*, 1996, **96**, 2983; (*b*) S. Gambarotta and J. Scott, *Angew. Chem., Int. Ed.*, 2004, **43**, 5298; (*c*) B. M. Hoffman, D. R. Dean and L. C. Seefeldt, *Acc. Chem. Res.*, 2009, **42**, 609.
8 (*a*) D. Sellmann, G. H. Rackelmann and F. W. Heinemann, *Chem.–Eur. J.*, 1997, **3**, 2071; (*b*) D. Sellmann and A. Fursattel, *Angew. Chem., Int. Ed.*, 1999, **38**, 2023.
9 (*a*) S. Park, A. J. Lough and R. H. Morris, *Inorg. Chem.*, 1996, **35**, 3001; (*b*) A. J. Lough, S. Park, R. Ramachandran and R. H. Morris, *J. Am. Chem. Soc.*, 1994, **116**, 8356.
10 E. Peris, J. C. Lee, J. R. Rambo, O. Eisenstein and R. H. Crabtree, *J. Am. Chem. Soc.*, 1995, **117**, 3485.
11 (*a*) R. C. Linck, R. J. Pafford and T. B. Rauchfuss, *J. Am. Chem. Soc.*, 2001, **123**, 8856; (*b*) C. Mealli and T. B. Rauchfuss, *Angew. Chem., Int. Ed.*, 2007, **46**, 8942.
12 S. Ogo, *Chem. Commun.*, 2009, 3317–3325.
13 (*a*) D. H. Lee, B. P. Patel, E. Clot, O. Eisenstein and R. H. Crabtree, *J. Chem. Soc., Chem. Commun.*, 1999, 297; (*b*) K. Gruet, E. Clot, O. Eisenstein, D. H. Lee, B. Patel, A. Macchioni and R. H. Crabtree, *New J. Chem.*, 2003, **27**, 80; (*c*) T. Liu, S. Chen, M. J. O'Hagan, M. Rakowski DuBois, R. M. Bullock and D. L. DuBois, *J. Am. Chem. Soc.*, 2012, **134**, 6257.
14 A. Llamazares, H. W. Schmalle and H. Berke, *Organometallics*, 2001, **20**, 5277.
15 N. V. Belkova, L. M. Epstein and E. S. Shubina, *Eur. J. Inorg. Chem.*, 2010, 3555.
16 C. P. Lau, S. M. Ng, G. Jia and Z. Lin, *Coord. Chem. Rev.*, 2007, **251**, 2223.
17 R. Custelcean and J. E. Jackson, *Chem. Rev.*, 2001, **101**, 1963.
18 R. H. Crabtree, P. E. Siegbahn, O. Eisenstein, A. L. Rheingold and T. F. Koetzle, *Acc. Chem. Res.*, 1996, **29**, 384.
19 (*a*) J. A. Ayllon, C. Gervaux, S. Sabo-Etienne and B. Chaudret, *Organometallics*, 1997, **16**, 2000; (*b*) Y. Guari, J. A. Ayllon, S. Sabo-Etienne and B. Chaudret, *Inorg. Chem.*, 1998, **37**, 640.
20 (*a*) E. S. Shubina, N. V. Belkova, E. V. Bakhmutova, E. V. Vorontsov, V. I. Bakhmutov, A. V. Ionidis, C. Bianchini, L. Marvelli, M. Peruzzini and L. M. Epstein, *Inorg. Chim. Acta*, 1998, **280**, 302; (*b*) N. V. Belkova, P. A. Dub, M. Baya and J. Houghton, *Inorg. Chim. Acta*, 2007, **360**, 149.
21 S. H. Park, A. J. Lough, G. P. A. Yap and R. H. Morris, *J. Organomet. Chem.*, 2000, **609**, 110.
22 M. Kranenburg, Y. E. M. van der Burgt, P. C. J. Kamer, P. W. N. M. van Leeuwen, K. Goubitz and J. Fraanje, *Organometallics*, 1995, **14**, 3081.
23 (*a*) P. W. N. M. van Leeuwen, P. C. J. Kamer, J. N. H. Reek and P. Dierkes, *Chem. Rev.*, 2000, **100**, 2741; (*b*) M.-N. Birkholz, Z. Freixa and P. W. N. M. van Leeuwen, *Chem. Soc. Rev.*, 2009, **38**, 1099.
24 (*a*) P. C. J. Kamer, P. W. N. M. van Leeuwen and J. N. H. Reek, *Acc. Chem. Res.*, 2001, **34**, 895; (*b*) J. A. Gillespie, D. L. Dodds and P. C. J. Kamer, *Dalton Trans.*, 2010, **39**, 2751.
25 P. Espinet and K. Soulantica, *Coord. Chem. Rev.*, 1999, **193–195**, 499.
26 Z.-Z. Zhang and H. Cheng, *Chem. Rev.*, 1996, **147**, 1.
27 F. A. Jalón, B. R. Manzano, A. Caballero, M. C. Carrion, L. Santos, G. Espino and M. Moreno, *J. Am. Chem. Soc.*, 2005, **127**, 15364.
28 D. B. Grotjahn, *Dalton Trans.*, 2008, 6497–6508.
29 (*a*) R. Noyori and T. Ohkuma, *Angew. Chem., Int. Ed.*, 2001, **40**, 40; (*b*) C. P. Casey, J. B. Johnson, S. W. Singer and Q. Cui, *J. Am. Chem. Soc.*, 2005, **127**, 3100.
30 (*a*) P. W. N. M. van Leeuwen, C. F. Roobeek, R. L. Wife and J. H. G. Frijns, *J. Chem. Soc., Chem. Commun.*, 1986, 31; (*b*) P. W. N. M. van Leeuwen and C. F. Roobeek, *New J. Chem.*, 1990, **14**, 487; (*c*) P. M. Castro, H. Gulyas, J. Benet-Buchholz, C. Bo, Z. Freixa and P. W. N. M. van Leeuwen, *Catal. Sci. Technol.*, 2011, **1**, 401.

31 (*a*) G. D. Frey, B. Lavallo, B. Donnadieu, W. W. Schoeller and G. Bertrand, *Science*, 2007, **316**, 439; (*b*) A. L. Kenward and W. E. Piers, *Angew. Chem., Int. Ed.*, 2008, **47**, 38; (*c*) D. Stephan and G. Erker, *Angew. Chem., Int. Ed.*, 2010, **49**, 46.
32 C. A. Casey and G. T. Whiteker, *Isr. J. Chem.*, 1990, **30**, 299.
33 P. Dierkes and P. W. N. M. van Leeuwen, *J. Chem. Soc., Dalton Trans.*, 1999, **10**, 1519.
34 P. E. Garrou, *Chem. Rev.*, 1981, **81**, 229.
35 T. G. Appleton, M. A. Bennet and I. B. Tomkins, *J. Chem. Soc., Dalton Trans.*, 1976, 439.
36 A. J. Deeming and M. B. Smith, *J. Chem. Soc., Dalton Trans.*, 1993, 3383.
37 D. Drommi, C. G. Arena, F. Nicolo, G. Bruno and F. Faraone, *J. Organomet. Chem.*, 1995, **485**, 115.
38 R. P. Schutte, S. J. Retting, A. M. Joshi and B. R. James, *Inorg. Chem.*, 1997, **36**, 5809.
39 M. Sato, H. Shigeta, M. Sekino and S. Akabori, *J. Organomet. Chem.*, 1993, **458**, 199.
40 T. G. Appleton and M. A. Bennet, *Inorg. Chem.*, 1978, **17**, 738.
41 M. A. Zuideveld, B. H. G. Swennenhuis, M. D. K. Boele, Y. Guari, G. P. F. van Strijdonck, J. N. H. Reek, P. C. J. Kamer, K. Goubitz, J. Fraanje, M. Lutz, A. L. Spek and P. W. N. M. van Leeuwen, *J. Chem. Soc., Dalton Trans.*, 2002, 2308.
42 A. J. Sandee, L. A. van der Veen, J. N. H. Reek, P. C. J. Kamer, M. Lutz, A. L. Spek and P. W. N. M. Van Leeuwen, *Angew. Chem., Int. Ed.*, 1999, **38**, 3231.
43 J. Yin and S. L. Buchwald, *J. Am. Chem. Soc.*, 2002, **124**, 6043.
44 L. D. Julian and J. F. Hartwig, *J. Am. Chem. Soc.*, 2010, **132**, 13813.
45 R. Dallanegra, A. B. Chaplin and A. S. Weller, *Organometallics*, 2012, **31**, 2720.
46 R. J. Pawley, M. A. Huertos, G. C. Lloyd-Jones, A. S. Weller and M. C. Willis, *Organometallics*, 2012, **31**, 5650.
47 A. Dervisi, P. G. Edwards, P. D. Newman, R. P. Tooze, S. J. Coles and M. B. Hursthouse, *J. Chem. Soc., Dalton Trans.*, 1998, 3771.
48 R. J. van Haaren, H. Oevering, B. B. Coussens, G. P. F. van Strijdonck, J. N. H. Reek, P. C. J. Kamer and P. W. N. M. van Leeuwen, *Eur. J. Inorg. Chem.*, 1999, 1237.
49 J. P. Farr, M. M. Olmstead, F. E. Wood and A. L. Balch, *J. Am. Chem. Soc.*, 1983, **105**, 792.
50 V. K. Jain, V. S. Jakkal and R. Bohra, *J. Organomet. Chem.*, 1990, **389**, 417.
51 M. M. Olmstead, A. Maisonnat, J. P. Farr and A. L. Balch, *Inorg. Chem.*, 1981, **20**, 4060.
52 T. Suzuki, M. Kita, K. Kashiwabara and J. Fujita, *Bull. Chem. Soc. Jpn.*, 1990, **63**, 3434.
53 L. A. van der Veen, P. H. Keeven, G. C. Schoemaker, J. N. H. Reek, P. C. J. Kamer, P. W. N. M. van Leeuwen, M. Lutz and A. L. Spek, *Organometallics*, 2000, **19**, 872.
54 R. J. van Haaren, K. Goubitz, J. Fraanje, G. P. F. van Strijdonck, H. Oevering, B. Coussens, J. N. H. Reek, P. C. J. Kamer and P. W. N. M. van Leeuwen, *Inorg. Chem.*, 2001, **40**, 3363.
55 M. A. Zuideveld, B. H. G. Swennenhuis, M. D. K. Boele, Y. Guari, G. P. F. van Strijdonck, J. N. H. Reek, P. C. J. Kamer, K. Goubitz, J. Fraanje, M. Lutz, A. L. Spek and P. W. N. M. van Leeuwen, *J. Chem. Soc., Dalton Trans.*, 2002, 2308–2317.
56 S. Okeya, T. Miyamoto, S. Oot, Y. Nakamura and S. Kawaguchi, *Bull. Chem. Soc. Jpn.*, 1984, **57**, 395.
57 M. J. Green, G. J. P. Britovsek, K. J. Cavell, W. Skelton and A. H. J. White, *Chem. Commun.*, 1996, 1563.
58 A. R. Siedle, R. A. Newmark and L. H. Pignolet, *J. Am. Chem. Soc.*, 1982, **104**, 6584.
59 M. Albrecht, P. Dani, M. Lutz, A. L. Spek and G. van Koten, *J. Am. Chem. Soc.*, 2000, **122**, 11822.
60 E. Drent and P. H. M. Budzelaar, *J. Organomet. Chem.*, 2000, **593**, 211.
61 D. Konya, K. Q. Almeida-Leñero and E. Drent, *Organometallics*, 2006, **25**, 3166.
62 P. Pelagatti, A. Bacchi, M. Carcelli, M. Costa, A. Fochi, P. Ghidini, E. Leporati, M. Masi, C. Pelizzi and G. Pelizzi, *J. Organomet. Chem.*, 1999, **583**, 94.
63 V. V. Grushin, *Chem. Rev.*, 1996, **96**, 2011.
64 E. G. Hope, W. Levason and N. A. Powell, *Inorg. Chim. Acta*, 1986, **115**, 187.
65 P. L. Goggin, R. J. Goodfellow, S. R. Haddock, B. F. Taylor and I. R. H. Marshall, *J. Chem. Soc., Dalton Trans.*, 1976, 459.
66 J. F. Hartwig, *Organotransition Metal Chemistry, From Bonding to Catalysis*, University Science Books, Sausolita, CA, 2010, ch. 3.
67 E. Alvarez, S. Conejero, M. Paneque, A. Petronilho, M. L. Poveda, O. Serrano and E. Carmona, *J. Am. Chem. Soc.*, 2006, **128**, 13060; S. Conejero, J. López-Serrano, M. Paneque, A. Petronilho, M. L. Poveda, F. Vattier, E. Alvarez and E. Carmona, *Chem.–Eur. J.*, 2012, **18**, 4644.
68 F. E. Goodson, T. I. Wallow and B. M. Novak, *J. Am. Chem. Soc.*, 1997, **119**, 12441.
69 P. W. N. M. van Leeuwen, *Appl. Catal., A*, 2001, **212**, 61.
70 P. W. N. M. van Leeuwen and J. C. Chadwick, *Homogeneous Catalysts: Activity, Stability, Deactivation*, Wiley-VCH, Weinheim, 2011, ch. 1 and 9.
71 M. L. H. Green, M. J. Smith, H. Felkin and G. Swierczewski, *J. Chem. Soc. D*, 1971, 158.
72 V. V. Grushin, *Organometallics*, 2000, **19**, 1888.
73 W. J. Marshall and V. V. Grushin, *Organometallics*, 2003, **22**, 555.
74 T. J. Geldbach, P. S. Pregosin and A. Albinati, *Organometallics*, 2003, **22**, 1443.
75 D. K. Morita, J. K. Stille and J. R. Norton, *J. Am. Chem. Soc.*, 1995, **117**, 8576.
76 A. Togni and T. Hayashi, *Ferrocenes*, Wiley, Weinheim, 1995.

77 T. Koizumi, K. Osakada and T. Yamamoto, *Organometallics*, 1997, **16**, 6014.
78 M. Hackett, J. A. Ibers and G. M. Whitesides, *J. Am. Chem. Soc.*, 1988, **110**, 1436.
79 M. Y. Chiang, R. Bau, G. Minghetti, A. L. Bandini, G. Banditelli and T. F. Koetzle, *Inorg. Chem.*, 1984, **23**, 122.
80 G. R. Newkome and D. C. Hager, *J. Org. Chem.*, 1978, **43**, 947.
81 F. R. Hartley, S. Murray and C. A. McAuliffe, *Inorg. Chem.*, 1979, **18**, 1394.
82 M. Hovorka and J. Zavada, *Org. Prep. Proced. Int.*, 1991, **23**, 200.
83 M. Brookhart, B. Grant and A. F. Volpe Jr, *Organometallics*, 1992, **11**, 3920.